I.O.S.

DEVELOPMENT OF STORM-SURGE MODELS AT BIDSTON

N. S. HEAPS

REPORT NO. 53

1977

NATURAL ENVIRONMENT RESEARCH COUNCIL

INSTITUTE OF OCEANOGRAPHIC SCIENCES

INSTITUTE OF OCEANOGRAPHIC SCIENCES

Wormley, Godalming
Surrey, GU8 5UB.
(0428 - 79 - 4141)
(Director: Professor H. Charnock)

Bidston Observatory,
Birkenhead,
Merseyside, L43 7RA.
(051 - 653 - 8633)
Assistant Director: Dr. D. E. Cartwright)

Crossway,
Taunton,
Somerset, TA1 2DW.
(0823 - 86211)
(Assistant Director: M. J. Tucker)

Marine Scientific Equipment Service
Research Vessel Base,
No. 1 Dock,
Barry,
South Glamorgan, CF6 6UZ.
(0446 - 737451)
(Officer-in-Charge: Dr. L. M. Skinner)

On citing this report in a bibliography the reference should be followed by the words UNPUBLISHED MANUSCRIPT.

Printed by The Natural Environment Research Council Office Services

DEVELOPMENT OF STORM-SURGE MODELS AT BIDSTON

N. S. HEAPS

REPORT NO. 53

1977

Institute of Oceanographic Sciences
Bidston Observatory
Birkenhead
Merseyside L43 7RA

CONTENTS

SUMMARY

This paper reviews the storm-surge numerical modelling work carried out at Bidston Observatory over a period of about ten years up to September 1977. Various stages in the development are described and the main purpose is to demonstrate the underlying strategy and direction of the work as well as to show specific results obtained from it. The programme of investigation is by no means complete, but a point has been reached when the foundations of a future real-time surge forecasting scheme for the North Sea, based on dynamical principles, appear to have been laid. Forecasting surge levels for the North Sea and the Thames Estuary has been central throughout, mainly due to its great practical importance in relation to coastal flooding and navigational problems. However, the models which have been developed extend over the entire continental shelf surrounding the British Isles, as well as concentrating on the North Sea basin itself, the Southern Bight of the North Sea, and the River Thames. The most significant advances have been made during the last three or four years as suitable meteorological data for driving the models has become more readily available. Results of the more recent numerical computations are given to illustrate the effectiveness of the approach in simulating actual storm-surge heights.

1. INTRODUCTION

This paper surveys the work done on storm-surge models at Bidston during the last ten years or so, relating to the problem of predicting storm surges in the North Sea and other areas on the North West European Continental Shelf. Investigations started with the formulation of a linear two-dimensional shelf model for basic studies of surge propagation in the North Sea. This was followed by a study of nonlinear surge-tide interaction in the southern North Sea and Thames Estuary using a combined two-dimensional sea model and one-dimensional river model. During the last four years investigations into the use of models for the purposes of surge prediction have intensified considerably with the availability of suitable meteorological forecasts from the 10-level model of the atmosphere at the Meteorological Office. The shelf model and a North Sea model of finer mesh have been developed to run with the latest meteorological data and real-time forecasting experiments are planned to take place within the next twelve months. A new model of the southern North Sea and River Thames is being proved which can provide predictions of sea level in the River for the operation of the future Thames Barrier. The situation is one of advancing achievement and the essentials of a practical surge forecasting system appear to have been established.

2. LINEAR SHELF MODEL

The first two-dimensional storm-surge model at Bidston, described by Heaps (1969), was based on the linearized hydrodynamic equations:

$$\frac{\partial \zeta}{\partial t} + \frac{1}{a\cos\phi}\left\{\frac{\partial}{\partial \phi}(U\cos\phi) + \frac{\partial V}{\partial \chi}\right\} = 0 , \qquad (1)$$

$$\frac{\partial U}{\partial t} + 2\omega\sin\phi\, V = -\frac{gh}{a}\frac{\partial \zeta}{\partial \phi} - \frac{h}{\rho a}\frac{\partial p_a}{\partial \phi} + \frac{1}{\rho}(F_s - F_B) , \qquad (2)$$

$$\frac{\partial V}{\partial t} - 2\omega\sin\phi\, U = -\frac{gh}{a\cos\phi}\frac{\partial \zeta}{\partial \chi} - \frac{h}{\rho a\cos\phi}\frac{\partial p_a}{\partial \chi} + \frac{1}{\rho}(G_s - G_B) , \qquad (3)$$

where the notation is :

ϕ, χ north latitude and east longitude,

t time,

ζ elevation of the sea surface,

U, V components of the total stream, to the north and to the east,

F_s, G_s components of the friction of the wind on the sea,

F_B, G_B components of the friction of the water on the sea bottom,

p_a atmospheric pressure on the sea,

h undisturbed depth of water,

ρ density of the water, assumed uniform,

a mean radius of the Earth,

g acceleration of the Earth's gravity,

ω angular speed of the Earth's rotation.

With bottom friction defined by

$$F_B = \lambda\rho U , \quad G_B = \lambda\rho V \quad (\lambda = \kappa/h , \ \kappa = 0{\cdot}24 \text{ cm/s}) \qquad (4)$$

and taking

$$\partial p_a/\partial \phi = \partial p_a/\partial \chi = 0 , \qquad (5)$$

finite difference solutions of (1), (2), (3) yielded the wind-generated surge ζ over areas of the North West European Continental Shelf corresponding to models 1, 2 and 3 delineated in figure 1. Model 1 with the Strait of Dover closed covers the

North Sea and shelf areas to the north and west of Scotland, model 2 covers the entire continental shelf, and model 3 extends over the whole shelf taking in an area of adjoining ocean in the north-west. The finite difference grid for model 2 is shown in figure 2 with ζ evaluated at the circle points and U, V at the cross points. For each model, the mesh size $(\Delta\phi, \Delta\chi)$ is such that $\Delta\phi = 1/3^\circ$, $\Delta\chi = 1/2^\circ$. Satisfying the condition of zero normal flow across land boundaries, and setting surge elevation permanently to zero along the open boundary (contiguous with the ocean), wind surges were computed through time by stepping forward from a supposed initial state of no motion (time step 0.1 hour for models 1 and 2, 0.05 hour for model 3); the presence of friction, mainly in the shallow coastal waters, damps down unreal transients created initially, which are in any case small compared with the effects of the wind forcing. The difference scheme was explicit, employing forward and backward differences in time and central differences in space.

Sub-areas used in specifying wind conditions over the respective models are shown in figure 1. The areas - which correspond to those employed by the Meteorological Office (M.O.) for weather forecasts - are numbered as indicated. As input data for surge calculations, surface winds over the different areas were determined for consecutive 2-hour intervals. The wind data was prepared by the M.O. by extracting geostrophic winds from 1:3,000,000 hourly weather charts of the British Isles : the geostrophic winds were then adjusted to surface winds by using results obtained by Findlater et al. (1966). Final estimates of the surface values took into consideration ships observations and a few land observations, particularly on occasions when the curvature of the

isobars appeared to be significant. Wind stress, F dyn/cm^2, on the sea surface was deduced from the surface wind, V_1 m/s, employing the square law

$$F = 12{\cdot}5\, c_D\, V_1^2 \tag{6}$$

with drag coefficient c_D given by

$$\left.\begin{aligned} 10^3 c_D &= 0{\cdot}554 && V_1 \leqslant 4{\cdot}917 \\ &= -0{\cdot}12 + 0{\cdot}137 V_1 && 4{\cdot}917 \leqslant V_1 \leqslant 19{\cdot}221 \\ &= 2{\cdot}513 && V_1 \geqslant 19{\cdot}221 \end{aligned}\right\} \tag{7}$$

The relevance of the sea-model calculations to the problem of calculating the variations in sea level at a coastal site is shown in figure 3. The total elevation of the sea surface was assumed to consist of the predicted tide ζ_T, the wind surge ζ_W derived from the computations, and the barometric surge ζ_B estimated from the statical law. Non-linear interactions of tide and surge were therefore ignored, as were the dynamic effects produced by changes in barometric pressure over the sea.

The sea models were used for research into the generation and propagation of different types of North Sea surge. To this end, wind induced elevations were evaluated for three surge periods :

(a) 0600, 13 September - 1200, 15 September : 1956,
(b) 1200, 24 February - 1800, 26 February : 1958,
(c) 0000, 15 February - 0000, 18 February : 1962.

Here, (a) represented a typical external surge in the North Sea and a principal aim of the investigation was to examine the origins of such surges, (b) represented an internal surge largely confined to the southern North Sea, while (c) contained a major North Sea surge - exceeding a height of 3.3 m at Hamburg. The weather charts and a comparison of computed and observed surges are shown in figures 4

and 5 for the surge case (c).

Experiments were carried out using the "influence" method of storm-surge computation in which, at two-hourly intervals, standard elevation responses to unit wind stress fields over the areas 1-17 (figure 1) were combined linearly in proportion to the actual stresses acting over these respective areas. However, the approach proved too inflexible in a situation of continuing model development.

3. MODEL OF THE SOUTHERN NORTH SEA AND THAMES ESTUARY

For a more detailed examination of storm-surge effects in the southern North Sea and River Thames, Banks (1974) formulated a two-dimensional fine-mesh model of this sea area ($\Delta\phi = 4/60^{o}$, $\Delta\chi = 6.8/60^{o}$) linked dynamically to a one-dimensional model of the river (section spacing : 4.9 miles). The system is illustrated in figure 6. The two-dimensional hydrodynamic equations consisted of (1), (2), (3) with h replaced by $h+\zeta$ and bottom stress expressed in terms of a quadratic law :

$$F_B = \frac{k\rho U(U^2+V^2)^{1/2}}{(h+\zeta)^2} \quad , \quad G_B = \frac{k\rho V(U^2+V^2)^{1/2}}{(h+\zeta)^2} \quad . \qquad (8)$$

Thus, the equations for the sea area were non-linear in so far as they included quadratic friction and allowed for time variations in the total depth of water. The equations for the river were similarly non-linear enhanced by the inclusion of a convective term. The finite difference scheme for the sea was basically that of the shelf model discussed in § 2, while the difference scheme for the river corresponded to that due to Rossiter and Lennon (1965).

The major 'Hamburg' surge of 15-17 February 1962 was simulated numerically applying the M_2 tide and surge elevations computed by

the shelf model along each open-sea boundary. Wind stress, derived as before, acted over the sea surface. Elevation ζ_{T+S} due to tide and surge combined was thereby generated throughout the model and, in separate runs, tide alone (no wind or boundary surge input) giving elevation ζ_T , and surge alone (no boundary tidal input) giving elevation ζ_S , were also computed. Satisfactory agreement was obtained between the computed wind surge with interaction $\zeta_{S+I} = \zeta_{T+S} - \zeta_T$ and the observed residual elevation after removal of the barometric surge. The comparison for Southend is given in figure 7 where the wind surge computed without the tide is also shown. Clearly, non-linear interaction between tide and surge produces two significant surge peaks out of one. This result demonstrates the importance of surge-tide interaction on surge levels in the southern North Sea and River Thames: models must include both tide and non-linear terms adequately to take proper account of the phenomenon.

A more recent hydrodynamic numerical model of the southern North Sea and River Thames, due to Prandle (1975), has a grid network extending through the Strait of Dover into the English Channel as indicated in figure 8. The disastrous surge of 31 January and 1 February 1953 was reproduced satisfactorily by this model specifying tide and surge from earlier estimates along the open boundaries. Both wind stress and atmospheric pressure gradient were included as forcing terms in the equations of motion - non-linear as above. The role of flow through the Strait of Dover in modifying surge levels in the Southern Bight was examined and the effects of Thames barrier closure on water levels along the river (figure 9) were determined. The total surge was analysed

into four components due respectively to the external surge entering across the northern boundary, the external surge entering across the southern boundary, wind stress, and atmospheric pressure gradient.

In a future surge prediction scheme, the latter model is envisaged as a more detailed part of the overall shelf-model configuration, receiving open-boundary information from the shelf model and running concurrently with it in the same operation. However, the model of the Bight may also be run independently, using observed tidal data on its open boundaries, and still provide a useful 6-hour surge prediction in the Thames for the purposes of barrier closure. Observational data on the open boundaries might ultimately be incorporated into an updating procedure in the combined running of the outer and inner models.

4. SHELF MODEL : PRELIMINARY SCHEME FOR SURGE PREDICTION

Model 2 of the continental shelf, described in § 2, has been developed to run in conjunction with forecast meteorological data obtained from the Bushby-Timpson 10-level atmosphere model on a fine mesh (Benwell et al. 1971) to provide a scheme for surge prediction. The first stage in this development, carried out by Flather and Davies (1975, 1976), is now outlined. The hydrodynamic equations were considered in the form :

$$\frac{\partial \zeta}{\partial t} + \frac{1}{a\cos\phi}\left\{ \frac{\partial}{\partial \chi}\left[(h+\zeta)u \right] + \frac{\partial}{\partial \phi}\left[(h+\zeta)v\cos\phi \right] \right\} = 0 , \quad (9)$$

$$\left.\begin{aligned} &\frac{\partial u}{\partial t} + \frac{u}{a\cos\phi}\frac{\partial u}{\partial \chi} + \frac{v}{a\cos\phi}\frac{\partial}{\partial \phi}(u\cos\phi) - 2\omega\sin\phi\, v \\ &\qquad = -\frac{g}{a\cos\phi}\frac{\partial \zeta}{\partial \chi} - \frac{1}{\rho a\cos\phi}\frac{\partial p_a}{\partial \chi} + \frac{F_S - F_B}{\rho(h+\zeta)} , \end{aligned}\right\} \quad (10)$$

$$\left.\begin{aligned} \frac{\partial v}{\partial t} + \frac{u}{a\cos\phi}\frac{\partial v}{\partial \chi} + \frac{v}{a}\frac{\partial v}{\partial \phi} + \frac{u^2\tan\phi}{a} + 2\omega\sin\phi\, u \\ = -\frac{g}{a}\frac{\partial \zeta}{\partial \phi} - \frac{1}{\rho a}\frac{\partial p_a}{\partial \phi} + \frac{G_s - G_B}{\rho(h+\zeta)} \end{aligned}\right\} \quad (11)$$

where u, v are components of depth-mean current directed to the east and to the north respectively and, consistent with (8),

$$F_B = k\rho u\left(u^2+v^2\right)^{1/2}, \qquad G_B = k\rho v\left(u^2+v^2\right)^{1/2}. \quad (12)$$

All the non-linear terms are included here; linearization and an inversion of component directions leads to the original set (1) - (4). Solutions of (9), (10), (11) were generated on the sea model grid with wind stress (F_s, G_s) and atmospheric pressure gradient $\partial p_a/\partial \chi$, $\partial p_a/\partial \phi$ estimated hourly from the height H of the 1000 millibar atmospheric pressure surface evaluated at the grid points of the meteorological model. The finite difference grids of the sea and the atmosphere models are shown superimposed in figure 10. As a first step, to simplify the computations, the convective terms were omitted from (10) and (11) and tides were excluded. Thus, in the notation already introduced, solutions yielded surge height ζ_s directly.

Grid lines in the sea model are lines of latitude spaced at $1/3^o$ and lines of longitude spaced at $1/2^o$, these forming the box elements shown in figure 10. For any such element, u is evaluated at the mid-points of the longitudinal sides, v at the mid-points of the latitudinal sides, and ζ at the centre of the box. The finite difference scheme, which advances ζ, u, v over the entire network at time t to the values of those variables at time $t+\Delta t$ is explicit : employing central space differences and a combination

of forward and backward time differences in the manner described by Flather and Heaps (1975). In generating the storm-surge fields, a time step Δt = 3 minutes was used. The boundaries and depth distribution of model 2 were assumed.

(a) Boundary conditions

Surges were generated from an initial state of rest at the start of the surge period, namely

$$\zeta = u = v = 0 \quad at \quad t = 0 \tag{13}$$

satisfying, along the model coastline, the condition that the normal component of current vanishes, i.e.

$$q_n = u \sin\beta + v \cos\beta = 0 \tag{14}$$

where β denotes the direction of the outward normal to the coast measured clockwise from the north. Several alternative conditions were used along the open sea boundary - which borders the Atlantic Ocean following approximately the 200 m depth contour. Thus, boundary elevation was specified as a function of position and time

$$\zeta = \hat{\zeta}(x, \phi, t) \tag{15}$$

with surge input $\hat{\zeta}$ estimated from the hydrostatic law :

$$\hat{\zeta} = (\bar{p}_a - p_a)/\rho g \quad , \tag{16}$$

$\bar{p}_a$ denoting a mean atmospheric pressure taken to be 1012 mb. A condition was also employed, relating ζ to q_n , which radiates internally generated disturbances outwards across the open boundary :

$$h(q_n - \hat{q}_n) = A(\zeta - \hat{\zeta}) \quad , \quad A = (gh)^{1/2}. \tag{17}$$

Here, $\hat{q}_n$ is the normal current associated with the input $\hat{\zeta}$: two cases were considered corresponding respectively to

$$\hat{q}_n = 0 \tag{18}$$

and

$$h\hat{q}_n = -A\hat{\zeta} . \tag{19}$$

(b) Meteorological data

The meteorological data for the sea model came from successive forecast runs of the M.O. 10-level model : a 36-hour forecast every 12 hours. Hourly values of the geopotential height H of the 1000 mb pressure surface at grid points covering the North West European Continental Shelf were stored on magnetic tape. Hours 6 to 18 of each forecast were selected giving a set of 13 spatial arrays of data spanning the 12-hour period covered.

The Cartesian system (x, y) , used as horizontal coordinates in the atmospheric model, is defined in terms of north-latitude and east-longitude using the stereographic map projection as follows :

$$\left.\begin{aligned} x &= \frac{2a}{a_1} \tan\left(\frac{\pi}{4} - \frac{\phi}{2}\right) \sin(\chi + 35^c) \\ y &= -\frac{2a}{a_1} \tan\left(\frac{\pi}{4} - \frac{\phi}{2}\right) \cos(\chi + 35^c) \end{aligned}\right\} \tag{20}$$

where $a_1/3$ is the grid length at the pole, so that x, y are dimensionless. The area covered by the stored data is contained within the rectangle whose sides are $x = 3\frac{1}{3}$, $x = 11$; $y = -6\frac{1}{3}$, $y = -14\frac{2}{3}$; mesh dimensions are $\Delta x = \Delta y = 1/3$. This gives an array of 24 x 26 point values of H each hour.

With

$$p_a = 1000\ mb + \rho_a g H \tag{21}$$

where ρ_a denotes the density of the air assumed uniform and constant in the vertical between the sea surface and the 1000 mb pressure surface, east and north gradients of atmospheric pressure become

$$\left.\begin{aligned} P &= \frac{1}{a\cos\phi}\frac{\partial p_a}{\partial \chi} = \frac{\rho_a g(1+\alpha^2)}{2\alpha a}\left\{ -y\frac{\partial H}{\partial x} + x\frac{\partial H}{\partial y}\right\}, \\ Q &= \frac{1}{a}\frac{\partial p_a}{\partial \phi} = -\frac{\rho_a g(1+\alpha^2)}{2\alpha a}\left\{ x\frac{\partial H}{\partial x} + y\frac{\partial H}{\partial y}\right\}, \end{aligned}\right\} \tag{22}$$

where $\alpha^2 = a_1^2(x^2+y^2)/4a^2$. Further, the components $(\hat{\omega}_\chi, \hat{\omega}_\phi)$ of the geostrophic wind at the sea surface are given by

$$\left.\begin{aligned} -2\omega\sin\phi\,\hat{\omega}_\phi &= -\frac{1}{\rho_a a\cos\phi}\frac{\partial p_a}{\partial \chi}, \\ 2\omega\sin\phi\,\hat{\omega}_\chi &= -\frac{1}{\rho_a a}\frac{\partial p_a}{\partial \phi}, \end{aligned}\right\} \tag{23}$$

whence

$$\left.\begin{aligned} \hat{\omega}_\chi &= -\frac{1}{2\omega\rho_a}\left\{(1+\alpha^2)/(1-\alpha^2)\right\} Q, \\ \hat{\omega}_\phi &= \frac{1}{2\omega\rho_a}\left\{(1+\alpha^2)/(1-\alpha^2)\right\} P. \end{aligned}\right\} \tag{24}$$

Replacing derivatives in (22) by centred differences, so that for example,

$$\partial H/\partial x = \left\{ H(x+\Delta x, y) - H(x-\Delta x, y)\right\}/2\Delta x \tag{25}$$

and using (24), numerical estimates of P, Q, $\hat{\omega}_\chi$ and $\hat{\omega}_\phi$ were obtained at grid points of the 10-level model within the rectangle

defined above. On the basis of work by Hasse and Wagner (1971), the magnitude of surface wind w was then calculated from that of the geostrophic wind $\hat{w}$ using the relation

$$w = 0.56\,\hat{w} + b \qquad (26)$$

taking $b = 2.4$ m/s. The directions of surface and geostrophic winds were assumed to be the same. The wind stress on the sea surface was subsequently deduced from (6) and (7).

The above formulae provided estimates of p_a, P, φ, F_s and G_s at grid points of the meteorological model. Interpolation carried out on the stereographic plane then gave P and F_s at each point (x_1, y_1) say, corresponding to a u-point (χ_1, ϕ_1); φ and G_s at each point corresponding to a v-point; and p_a at points corresponding to elevation points on the open boundary. This was the data needed for the surge calculations. The fields of wind stress and atmospheric pressure gradient were taken as constant over each hour-long interval centred on their time of estimation. However, atmospheric pressure p_a on the open boundary, for use in (16), was interpolated linearly through time between the hourly estimates.

(c) Surge computations

Two surge cases were considered corresponding to the periods 26-30 March 1972 and 28 March - 6 April 1973.

In the first case, surge levels on the east coast of Britain were relatively small but strong westerly and northwesterly winds acting over the North Sea raised water levels on the Dutch coast and in the German Bight by up to 120 cm producing a very broad surge peak. Separate computed runs were carried out with three different open-

boundary conditions based respectively on (15), (17) and (18), (17) and (19). The influence of the differing boundary condition on surge height was small in the interior of the North Sea but significant at the more northerly ports such as Stornoway and Bergen. Overall, the use of (17) and (18) gave the best results in comparisons with observations of residual elevation.

For the second case, the weather charts given in figure 11 indicate a series of fronts and depressions crossing the British Isles. In figures 12a and 12b, computed 15-minute values of surge height (continuous line) are compared with observed hourly values of residual elevation (discrete points) at ports around the North Sea. The computations used open boundary conditions (17) and (18). Clearly, the first surge peak on 2 and 3 April is reproduced fairly well except at Terschelling, Cuxhaven and Esbjerg where it is badly underestimated. However, the large negative surge which affected the east coast of England and the Southern Bight on 4 April is absent from the calculated surge profiles. These poor results may be associated with disturbances caused by the passage of a frontal system eastwards across the shelf on 4 and 5 April, accompanied by locally strong south or southwesterly winds; the wind direction changed rapidly across the fronts.

5. SHELF MODEL : MODIFIED SCHEME

In a series of numerical experiments with the shelf model, Flather (1976b) determined the sensitivity of the predicted surge to changes in certain procedures of the forecasting method. The purpose was to find out how the scheme might be modified to give more accurate results. The surge of 28 March - 6 April 1973, already discussed in §4, was used as a test case. Five further solutions for this event

were developed incorporating successive modifications. These are now described.

Solution A

Account was taken of the convective accelerations previously omitted in (10) and (11), and improvements were made in the model's representation of coastal configuration. Barriers were introduced to represent islands including the Isle of Man, the Hebrides, the Orkneys and the Shetlands. The entrance to the Skaggerak, previously treated as a coastal boundary, was changed into an open sea boundary.

Solution B

In the light of work by Hasse (1974) and Duun-Christensen (1971, 1975), the cross-isobar angle δ between the directions of the surface and geostrophic winds was taken as 20^{o} rather than 0^{o}. (This was done recognising the dependence of δ on frictional effects and the stability of the atmospheric boundary layer, in reality). Surface wind components $(\omega_\chi, \omega_\phi)$ were then determined from

$$\left.\begin{aligned} \omega_\chi &= (0.56\,\hat{\omega} + b)(\hat{\omega}_\chi \cos\delta - \hat{\omega}_\phi \sin\delta)/\hat{\omega}\,, \\ \omega_\phi &= (0.56\,\hat{\omega} + b)(\hat{\omega}_\chi \sin\delta + \hat{\omega}_\phi \cos\delta)/\hat{\omega}\,, \end{aligned}\right\} \qquad (27)$$

with

$$\hat{\omega} = (\hat{\omega}_\chi^2 + \hat{\omega}_\phi^2)^{1/2}\,, \quad b = 2{\cdot}4 \text{ m/s}\,. \qquad (28)$$

Solution C

To improve the estimates of atmospheric pressure gradient, spatial gradients of H originally evaluated using :

$$\left.\begin{aligned} (\partial H/\partial x)_{x,y} &\doteq \{ H(x+\Delta x, y) - H(x-\Delta x, y)\}/2\Delta x, \\ (\partial H/\partial y)_{x,y} &\doteq \{ H(x, y+\Delta y) - H(x, y-\Delta y)\}/2\Delta y, \end{aligned}\right\} \quad (29)$$

were re-determined in the revised forms :

$$\left.\begin{aligned} (\partial H/\partial x)_{x+\Delta x/2,\, y+\Delta y/2} &= \left\{ \begin{matrix} H(x+\Delta x, y+\Delta y) - H(x, y+\Delta y) \\ + H(x+\Delta x, y) - H(x,y) \end{matrix} \right\} \Big/ 2\Delta x, \\ (\partial H/\partial y)_{x+\Delta x/2,\, y+\Delta y/2} &= \left\{ \begin{matrix} H(x+\Delta x, y+\Delta y) - H(x+\Delta x, y) \\ + H(x, y+\Delta y) - H(x,y) \end{matrix} \right\} \Big/ 2\Delta y. \end{aligned}\right\} \quad (30)$$

Differences are taken over Δx ($\sim$ 100 km) in (30) rather than over $2\Delta x$ as in (29), giving a finer resolution of the derived wind field.

Solution D

In view of the importance of shallow water areas in tidal propagation and surge generation, a new set of depths for the sea model, with no artificial smoothing, was prepared from navigational charts. A revised solution, incorporating the new topography was then obtained.

Solution E

Two separate model runs were carried out for each forecast period: one to predict the tide alone (consisting of M_2 + S_2) and the other to predict tide and surge together.

The difference between these two solutions gave the surge prediction including the effects of surge-tide interaction. In order to introduce tide in addition to surge into the model, the condition applied on the open sea boundaries had to be altered.

In fact the following generalised form of (17) was used :

$$q_n = \hat{q}_n^{(s)} + \sum_i \hat{q}_n^{(i)} + \frac{A}{h}\left\{ \zeta - \hat{\zeta}^{(s)} - \sum_i \hat{\zeta}^{(i)} \right\} \qquad (31)$$

where $\hat{\zeta}^{(s)}$, $\hat{q}_n^{(s)}$ denote elevation and normal current input for the surge and $\hat{\zeta}^{(i)}$, $\hat{q}_n^{(i)}$ elevation and normal current input for the i th tidal constituent (i = 1,2 for the two constituents M_2 and S_2 considered). As before, in (16) and (18) :

$$\hat{\zeta}^{(s)} = \left(\bar{p}_a - p_a \right)/\rho g \quad , \quad \hat{q}_n^{(s)} = 0 \qquad (32)$$

while

$$\left.\begin{aligned} \hat{\zeta}^{(i)} &= f_i H_i \cos\left(\sigma_i t + V_i + u_i - g_i \right) , \\ \hat{q}_n^{(i)} &= f_i Q_i \cos\left(\sigma_i t + V_i + u_i - \gamma_i \right) , \end{aligned}\right\} \qquad (33)$$

where, for the i th constituent : H_i , g_i , Q_i , γ_i are known tidal constants (Flather 1976a), σ_i is the speed, f_i and u_i nodal factors, and V_i the phase of the corresponding elevation equilibrium constituent at Greenwich at time $t = 0$.

The sequence of modifications outlined above produced a significant reduction in the RMS errors in the computed surges at various North Sea ports, as shown in Table 1. Results from the final solution E are given in figures 13a and 13b, showing a marked improvement on the original solution represented by figures 12a and 12b. The negative surge on 4 April is now reproduced quite well.

As a further test of the modified scheme used in solution E, an extended prediction covering a period of 44 days was carried out. The period selected was 4 November to 18 December 1973, a particularly stormy time which included a number of large surges.

The weather charts show that most storms during the period were caused by rather similar meteorological events in which a large depression moved east or south-east from somewhere between Iceland and the Faroes subsequently crossing Southern Scandinavia and passing on into the Baltic. Results of computed surge height for British ports, compared with corresponding observed surge height, are shown in figures 14a, 14b, 14c and 14d. An accuracy comparable to that attained for the April surge period was maintained more or less throughout the entire period. One of the larger surges occurred on 19 November giving a maximum surge level of 210 cm at Southend. Determined from the computations : contours of surge elevation and the distribution of surge-current vectors at 1900 hours, preceding the main surge peak, are shown in figure 15. The currents are very substantial, attaining magnitudes similar to those of the strongest tidal flows.

6. PRACTICAL ASPECTS OF SURGE PREDICTION

Flather (1976c) has proposed a practical system for operational surge forecasting using meteorological data from the whole 36 hours of each 10-level model forecast. The scheme is illustrated in figure 16.

Numerical weather predictions using the 10-level model are carried out twice a day, each prediction run covering the period $0 \leqslant t_m \leqslant 36$ hours where t_m denotes meteorological model time and $t_m = 0$ corresponds to either 0000 GMT or 1200 GMT on the day. At say 0500 GMT or 1700 GMT, data for a surge calculation would be extracted from the output of the 10-level model and stored on magnetic tape. This data would comprise hourly arrays, for $7 \leqslant t_m \leqslant 36$ hours, of geopotential heights (H) of the 1000 mb

pressure surface at the shelf grid points of the atmospheric model. The data would, if necessary, be transferred from the magnetic tape on the computer at the M.O. to a similar magnetic tape on the computer at I.O.S. Bidston or wherever the surge prediction part of the process was to be carried out. The time required for data transmission would be of the order of 20 minutes so that the surge calculation could begin at say 0545 GMT or 1745 GMT.

Each sea model prediction run would cover a period of $0 \leqslant t_s \leqslant 29$ hours, where t_s denotes sea model time and $t_s = 0$ corresponds to $t_m = 7$ being either 0700 GMT or 1900 GMT on the day. The initial state of the sea would be taken directly from fields computed in the previous forecast with no input of observational information. Thus, referring to figure 16, the situation at time $t_s = 0$ in forecast 3 is identified with that at time $t_s = 12$ in forecast 2, stored in the preceding run. If, for some reason, forecast 2 were unavailable then fields from $t_s = 24$ in forecast 1 would be used as initial conditions for forecast 3. Thus, by storing data twice at $t_s = 12$ and $t_s = 24$ during each sea model run, the ongoing sequence of surge forecasts would survive interruption by the loss of a meteorological forecast. A surge forecast takes approximately 6 minutes processing time on the IBM 370/165 computer at Daresbury and, therefore, could be available for issue by about 0600 GMT or 1800 GMT.

Flather has tested the above scheme, as far as possible without facilities for the real time transmission of meteorological data and the necessary priority in accessing computers, by carrying out overlapping predictions for the period 10-21 November 1973. Twelve-hourly sea model forecasts, each extending over 29 hours, were

prepared. These experiments showed that, although errors increase when predicting further ahead, useful results can be obtained with meteorological data taken from the whole of each 36 hour numerical weather forecast. Worthwhile predictions of developing surges up to 30 hours in advance are therefore possible.

Tests were also carried out to simulate the effect on the surge predictions of the loss of one meteorological forecast at various times during the period 18-20 November 1973. Following an interruption, sea model calculations were continued as described above using as initial conditions data from t_s = 24 hours of the forecast before the one presumed lost. The results indicated that the influence of such an interruption is unlikely to extend beyond the first few hours of the following forecast, demonstrating the general practicability of the approach.

7. FINE MESH NUMERICAL MODEL OF THE NORTH SEA

Davies (1976a) has formulated a two-dimensional numerical model of the North Sea, again based on equations (9) - (12) discretized as in § 4, with a mesh resolution of $1/9^{o}$ latitude by $1/6^{o}$ longitude - compared with $1/3^{o}$ latitude by $1/2^{o}$ longitude for the coarser shelf model. The resolution is considerably finer than that used in earlier models of the North Sea, e.g. see Duun-Christensen (1971), allowing the shallow coastal regions to be modelled more accurately than hitherto. The finite difference grid, with lines coincident with the parallels and meridians of the shelf model, is illustrated in figure 17.

This North Sea model has been run in conjunction with the shelf model, employing solution E of § 5, for the surge periods : 28 March - 6 April 1973 (Davies and Flather 1977) and 4 November -

18 December 1973 (Davies 1976b). Results derived from the shelf model running alone for these periods have already been discussed. The estimation of wind stress and atmospheric pressure gradient for input to the North Sea model followed the same method used for the shelf model. On the open boundaries of the North Sea model (lying between Scotland and Norway in the north, and crossing the English Channel in the south : figure 17) a condition specifying elevation was satisfied, namely

$$\zeta = \hat{\zeta}^{(s)} + \sum_i \hat{\zeta}^{(i)} \qquad (34)$$

where $\hat{\zeta}^{(s)}$ denotes surge height and $\hat{\zeta}^{(i)}$ known elevation associated with tidal constituent i given as in (33). Again the tidal constituents M_2 and S_2 ($i = 1,2$) were considered. To evaluate $\hat{\zeta}^{(s)}$, elevation residuals computed by and taken from the shelf model were interpolated linearly along the North Sea model's open boundaries. Along the northern open boundary, use was made of observed residual elevations at Wick to adjust these input residuals. Thus, at any time, the residuals along the section of boundary between the Scottish coast and the Greenwich meridian were incremented by the difference between the observed and computed values at Wick linearly interpolated along the length of the section to a zero value at ($59^{o}20'W$, $0^{o}00'E$). The solution of surge with tide, obtained with (34), was diminished by the solution of tide only, obtained with (34) taking $\hat{\zeta}^{(s)} = 0$, to yield the storm surge solution.

The effect of introducing observations at Wick is demonstrated in the simulation of the surge of 19-20 November 1973. The shelf model

is in error by approximately 0.25 m at Wick at the surge peak and this error propagates into the North Sea, intensifying, and producing a surge peak error at Southend of over 0.5 m (figure 14b). Introducing observations at Wick into the North Sea model removed this error and the model yielded near perfect agreement between calculated and observed surge maxima along the east coast of England. Further, for the period 14-18 December 1973, the shelf model overestimated the surge at Wick by up to 40 cm. In these circumstances, a reduction of the order of 20 cm in the RMS errors in computed surge heights at North Sea ports was obtained from the North Sea model by inclusion of the Wick residuals. Figures 18a and 18b show the surge profiles derived from the shelf and North Sea models respectively for this period, with observed residuals also plotted. Evidently, for surges generated outside the North Sea which subsequently propagate into it across the northern boundary, small errors produced by the shelf model in the northern region can lead to significant errors in the Southern Bight. Introducing observational data along the open boundaries of the North Sea model is a means of reducing such errors. For internal storm surges, particularly those within the Southern Bight itself, both the shelf model and the North Sea model appear to give similar results; the dominant effect is then directly meteorological, external disturbances having a relatively insignificant influence.

Within the overall surge forecasting plan, the North Sea model may be regarded as a component part in a similar sense to the southern North Sea model of § 3, receiving open boundary information from the shelf model and from sea level observations. The model gives quite a detailed spatial description of surge elevations and

currents as shown for example by figure 19. The model was designed for the interpretation of observations taken during the JONSDAP 76 Oceanographic Experiment (figure 20) and will rely on those observations for the optimisation of its tidal and frictional parameters. A three-dimensional model is being formulated on the same grid network.

8. FURTHER DEVELOPMENTS : THE STORM SURGE OF JANUARY 1976

Recent development of the storm-surge prediction scheme, by R. A. Flather and A. M. Davies, has centred primarily on experiments employing different derivations of the meteorological input data required for both shelf and North Sea models. In this work, the storm surges during the period 31 December 1975 - 6 January 1976 have been simulated : a major surge peak of 2.67 metres was recorded at Southend on 3 January.

Figure 21, constructed by R. A. Flather, summarises the storm-surge calculations which have been carried out, indicating the various input-data derivations, the storm periods considered, and the models used - i.e. either the shelf model, S, or the North Sea model, N. Referring to figure 21, the following procedures were tried out.

In (A) : the meteorological data was derived as described in § 4 and § 5 using (27), (28) and (30) with $\delta = 20^{o}$. Pressure gradients ∇p_a and wind stress $\underset{\sim}{\tau}^{(s)}$ were estimated on the meteorological grid and then interpolated on to the sea model grids.

In (B) : sea surface pressure p_a , evaluated at the grid points of the meteorological model using (21), was interpolated on to the sea model grid points. Gradients ∇p_a and wind stress $\underset{\sim}{\tau}^{(s)}$ were then estimated from these interpolated values essentially as in (A).

Surges for 31 December 1975 - 6 January 1976 computed by model S using this technique are shown in figure 22.

In (C) : surface winds required for the calculation of wind stress $\underset{\sim}{\tau}^{(s)}$ were identified with the 1000 mb winds taken from the meteorological model. This led to an overestimation of the surge levels for 1-6 January 1976, with model S.

In (D) : surface wind w was estimated from the geostrophic wind $\hat{w}$ using the result of Hasse (1974) :

$$\left.\begin{aligned} w &= a\,\hat{w} + b \ , \\ a &= 0{\cdot}54 - 0{\cdot}012\,\Delta T_{a-s} \ , \\ b &= 1{\cdot}68 - 0{\cdot}105\,\Delta T_{a-s} \ (m/s) \ , \end{aligned}\right\} \qquad (35)$$

where $\Delta T_{a-s} = T_a - T_s$, T_s denoting sea surface temperature and T_a the temperature of the air directly above the sea surface (^{o}C). The cross-isobar angle δ was determined from a numerical function of ΔT_{a-s} given by Hasse (1974). The evaluation of T_a was based on a knowledge of h'_{950} the thickness of the layer between 900 and 1000 mb in the meteorological model : the average temperature of this layer $\overline{T}_{950}$ was deduced from h'_{950} and T_a then followed from $\overline{T}_{950}$ (^{o}K) assuming a dry adiabatic lapse rate. Values of T_s were taken from the Atlas : "Mean monthly temperature and salinity of the surface layer of the North Sea and adjacent waters from 1905 to 1954", published in 1962 by the International Council for the Exploration of the Sea. Computations with model S using this procedure tended to underestimate the surges of 1-6 January 1976.

In (E) : the drag coefficient c_D given by (7), used in all previous calculations, was replaced by a drag coefficient given by Smith & Banke (1975) :

$$10^3 C_D = 0.63 + 0.066\, w \qquad (36)$$

and experiment (C) was repeated. The surges computed thus, with model S, were not significantly different from those obtained in (C).

In (F) : the storm surge of 31 December 1975 - 6 January 1976 was computed as in (E) but using, where it was available, the NORSWAM meteorological data prepared by the Institute of Oceanographic Sciences in conjunction with the Meteorological Office. The NORSWAM data set contains time series of wind and pressure fields over the sea for some 42 severe storms occurring in the North Sea during the period 1966-1976. The wind and pressure fields are specified at 3 hourly intervals at the grid points of the 10-level model. The data is neither purely observational nor purely predicted in character, but was extracted painstakingly from synoptic charts and supplementary information. Results from model S are shown in figure 23, demonstrating the best agreement with observations obtained for the January 1976 storm surges. This emphasises the key role of accuracy in the meteorological data for the surge prediction scheme.

In (G), (H), (I) : the meteorological input data was derived as in (B), (C), (D) respectively. However, the calculations were based on sea surface pressure p_a , surface wind $\underset{\sim}{w}$ and air temperature T_a supplied by the M.O. on the basis of output from the meteorological model. Surges during the period 29 March - 2 April 1977 have been computed, with model S, using this data. It is anticipated that future experiments in real time surge prediction will employ the procedures (G), (H), or (I).

9. CONCLUDING REMARKS

During the last few years, numerical models have been under development at I.O.S. Bidston which attempt to simulate tide and surge motions in the North Sea and, indeed, over the entire North West European Shelf. The present paper has outlined the various stages of this development. It seems clear that these models are now sufficiently advanced in proved design to be considered as additional tools to be used in the real time prediction of sea level changes around our coasts, as well as providing information on such changes at off-shore positions distributed over the entire sea area surrounding the British Isles. The prediction of depth-averaged currents over this area also becomes possible adopting the modelling approach. Ultimately, the aim is to set up a comprehensive oceanographic prediction system, and this will require a link between research and forecasting activity in the future.

Present methods of real time prediction based on statistical correlations, albeit pressed to extreme limits of development, are limited in their range of application and there are doubts as to whether they can incorporate enough of the essential hydrodynamics of tides and surges for them to be reliable in the very severe, relatively infrequent, often unusual, storm situations. The introduction of computer models into the day to day prediction of surge levels, particularly relating to the east coast of England and the Thames Estuary, would take account of the complicated interactive and dynamic effects of tide with surge, significant in shallow waters and in rapidly changing weather situations. The use of the models would add a new

dimension of validity to the existing methods and, as already indicated, would extend the range of oceanographic factors which could be predicted. Output would cover both positive and negative surges since the complete time profile of sea level would be produced.

As a next stage of the work, three or four five-day periods are to be selected, separated by intervals of about a month, when meteorological forecast data, relayed twice-daily by telephone line from the Meteorological Office to the I.O.S. computer at Bidston, will be processed in real time to give surge predictions - also in real time. The main purpose will be to approach operational prediction conditions as near as possible in order to test the practical feasibility of a prediction scheme. The shelf model will be used exclusively at first, but the models of the "southern North Sea and Thames Estuary" and the "North Sea alone" are expected to be introduced as subsets later, giving more detailed results in specific areas of interest and providing predictions (e.g. for Thames Barrier operation) within the 12 hourly prediction system supported by the shelf model.

I am grateful to my colleagues, Dr. A. M. Davies, Dr. R. A. Flather, Dr. D. Prandle and Dr. J. E. Tranter for making their diagrams available to me for inclusion in this paper. Discussions with them on their work have been invaluable in preparing this summary of storm surge model development. My thanks are also due to Mr.R.A.Smith for help in the preparation of the diagrams.

REFERENCES

BANKS, J.E. 1974 A mathematical model of a river-shallow sea system used to investigate tide, surge and their interaction in the Thames - southern North Sea region. Philosophical Transactions of the Royal Society of London, A, 275, 567-609.

BENWELL, G.R.R., GADD, A.J., KEERS, J.F., TIMPSON, M.S. and WHITE, P.W. 1971 The Bushby-Timpson 10 level model on a fine mesh. Scientific Papers, Meteorological Office, London, 32, 23 pp.

DAVIES, A.M. 1976a A numerical model of the North Sea and its use in choosing locations for the deployment of offshore tide gauges in the JONSDAP '76 oceanographic experiment. Deutsche Hydrographische Zeitschrift, 29, 11-24.

DAVIES, A.M. 1976b Application of a fine mesh numerical model of the North Sea to the calculation of storm surge elevations and currents. Institute of Oceanographic Sciences, Report, No.28. 30 pp + figs.

DAVIES, A.M. & FLATHER, R.A. 1977 Computation of the storm surge of 1-6 April 1973 using numerical models of the North West European Continental Shelf and the North Sea. Deutsche Hydrographische Zeitschrift, 30, 139-162.

DUUN-CHRISTENSEN, J.C. 1971 Investigations on the practical use of a hydrodynamic numeric model for calculation of sea level variations in the North Sea, the Skaggerak and the Kattegat. Deutsche Hydrographische Zeitschrift, 24, 210-240.

DUUN-CHRISTENSEN, J.C. 1975 The representation of the surface pressure field in a two-dimensional hydrodynamic numeric model for the North Sea, the Skaggerak and the Kattegat. Deutsche Hydrographische Zeitschrift, 28, 97-116.

FINDLATER, J., HARROWER, T.N.S., HOWKINS, G.A. & WRIGHT, H.L. 1966 Surface and 900 mb wind relationships. Scientific Papers, Meteorological Office, London, 23, 41 pp.

FLATHER, R.A. 1976a A tidal model of the North-West European Continental Shelf. Mémoires de la Société royale de Liège, ser. 6, 10, 141-164.

FLATHER, R.A. 1976b Results from a storm surge prediction model of the North-West European Continental Shelf for April, November and December 1973. Institute of Oceanographic Sciences, Report, No.24. 37 pp + figs.

FLATHER, R.A. 1976c Practical aspects of the use of numerical models for surge prediction. Institute of Oceanographic Sciences, Report, No.30. 18 pp + figs.

FLATHER, R.A. & DAVIES, A.M. 1975 The application of numerical models to storm surge prediction. Institute of Oceanographic Sciences, Report, No.16. 22 pp + figs.

FLATHER, R.A. & DAVIES, A.M. 1976 Note on a preliminary scheme for storm surge prediction using numerical models. Quarterly Journal of the Royal Meteorological Society, 102, 123-132.

FLATHER, R.A. & HEAPS, N.S. 1975 Tidal computations for Morecambe Bay. Geophysical Journal of the Royal Astronomical Society, 42, 489-517.

HASSE, L. & WAGNER, V. 1971 On the relationship between geostrophic and surface wind at sea. Monthly Weather Review, 99, 255-260.

HASSE, L. 1974 On the surface to geostrophic wind relationship at sea and the stability dependence of the resistance law. Beitrage zur Physik der Atmosphäre, 45, 45-55.

HEAPS, N.S. 1969 A two-dimensional numerical sea model. Philosophical Transactions of the Royal Society of London, A, 265, 93-137.

PRANDLE, D. 1975 Storm surges in the southern North Sea and River Thames. Proceedings of the Royal Society of London, A, 344, 509-539.

ROSSITER, J.R. & LENNON, G.W. 1965 Computation of tidal conditions in the Thames Estuary by the initial-value method. Proceedings of the Institution of Civil Engineers, 31, 25-56.

SMITH, S.D. & BANKE, E.G. 1975 Variation of the sea surface drag coefficient with wind speed. Quarterly Journal of the Royal Meteorological Society, 101. 665-673.

Port	Run 0	Run A*	Run B	Run C	Run D	Run E
Wick	16.6	16.7	16.5	17.6	18.1	13.5
Aberdeen	21.4	21.8	19.5	20.3	20.3	15.9
North Shields	26.4	25.0	18.9	21.9	22.5	17.0
Inner Dowsing	39.4	34.4	27.3	26.0	26.9	21.2
Immingham	35.4	32.4	25.6	25.6	26.6	19.5
Lowestoft	45.0	38.2	28.9	27.4	29.8	25.0
Walton-on-Naze	50.6	45.3	37.8	33.3	34.3	27.2
Southend	60.8	50.6	47.5	41.5	42.9	33.9
Ostende	45.4	41.4	33.9	35.7	36.1	25.1
Ijmuiden	50.7	43.5	37.2	42.4	42.3	34.6
Terschelling	42.7	35.3	25.2	32.2	32.3	27.2
Cuxhaven	60.9	58.5	45.5	47.9	48.0	37.4
Esbjerg	40.8	45.5	33.7	32.1	32.6	23.3
Bergen	13.6	12.4	12.6	12.0	13.3	11.1

Table 1. RMS errors (cm) based on hourly values of computed and observed surge for the period 0700 2/4/73 - 1900 6/4/73.

(* period 0700 3/4/73 - 1900 6/4/73 only)

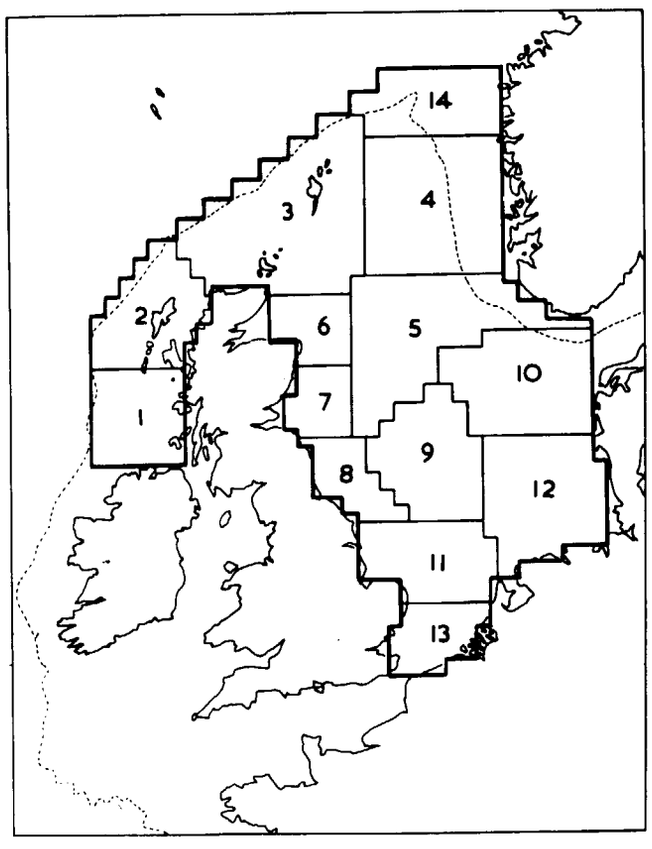

SUB-AREAS OF NORTH SEA MODEL 1

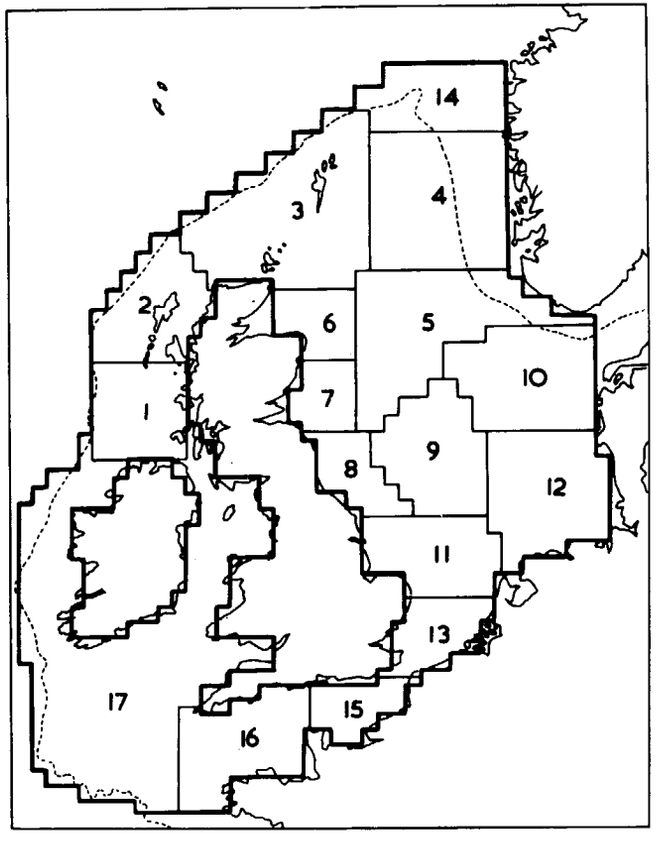

SUB-AREAS OF NORTH SEA MODEL 2

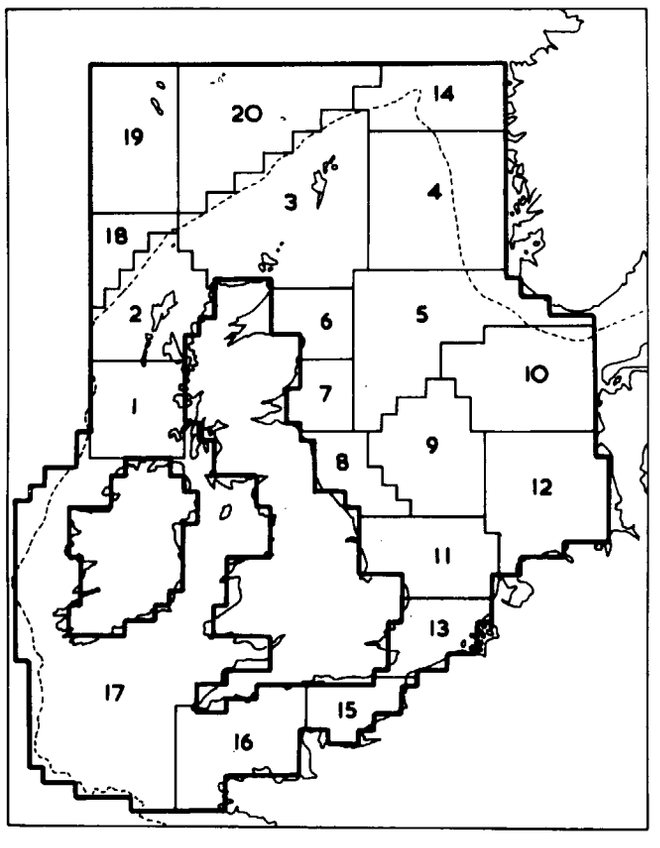

SUB-AREAS OF NORTH SEA MODEL 3

Figure 1: Sub-areas used in the specification of wind conditions over models 1,2 and 3.

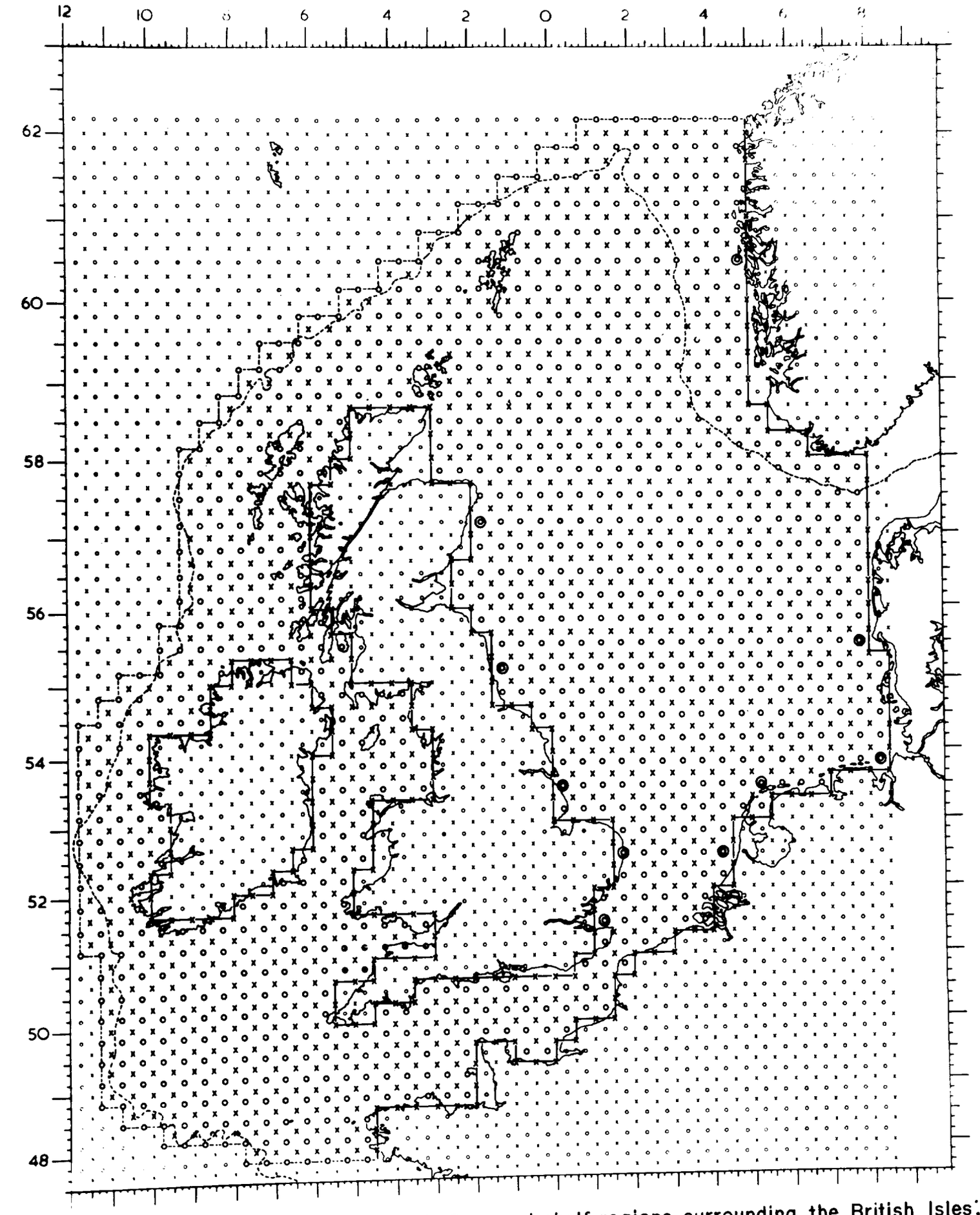

Figure 2: Model 2, covering the North Sea and shelf regions surrounding the British Isles; ——, open boundary; ——x——, closed boundary; - - - - - -, 100 fathoms; ◎, point at which calculated elevations are compared with elevations derived from observations at a nearby port.

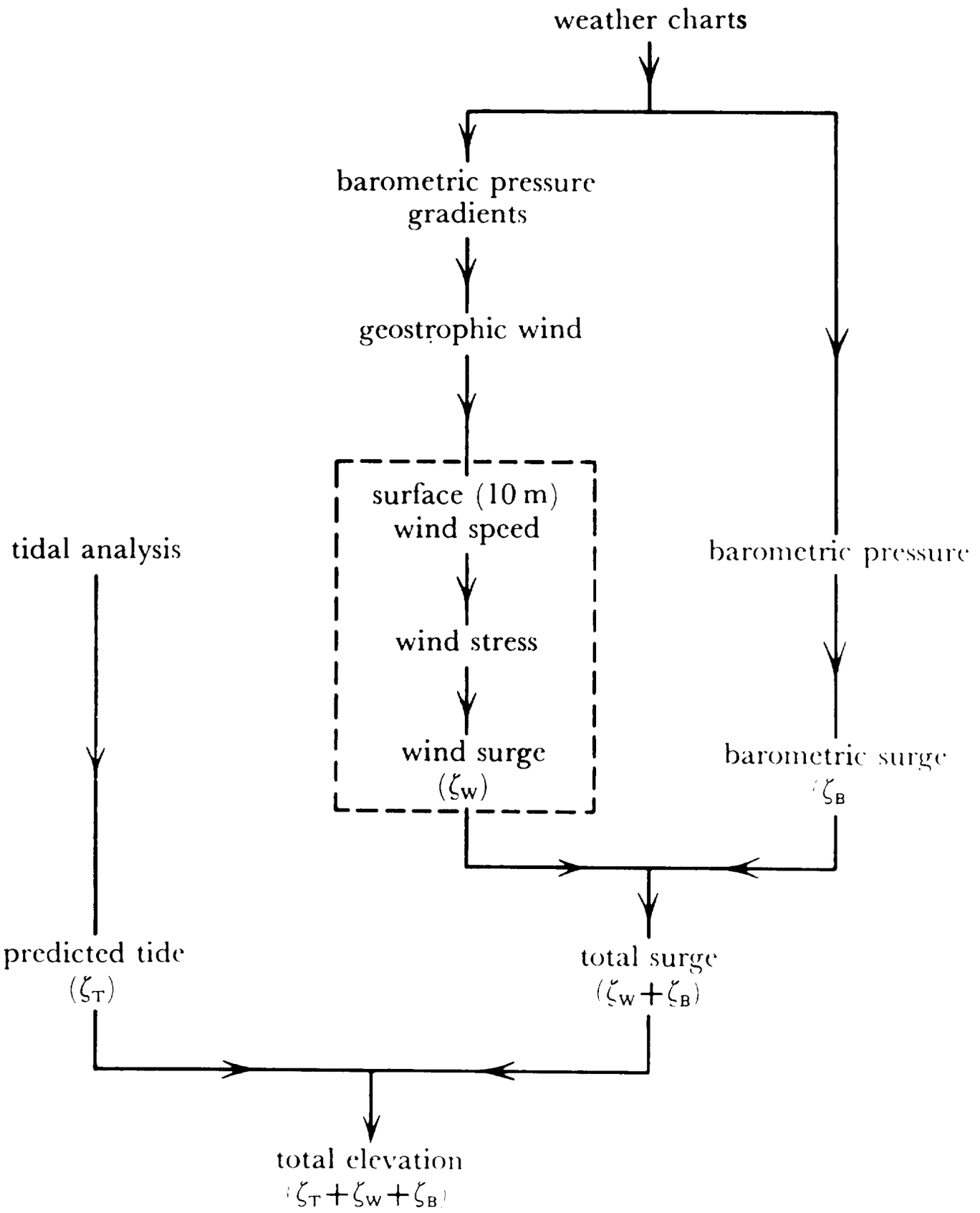

Figure 3: Scheme for calculating sea level; [------], sea-model computations.

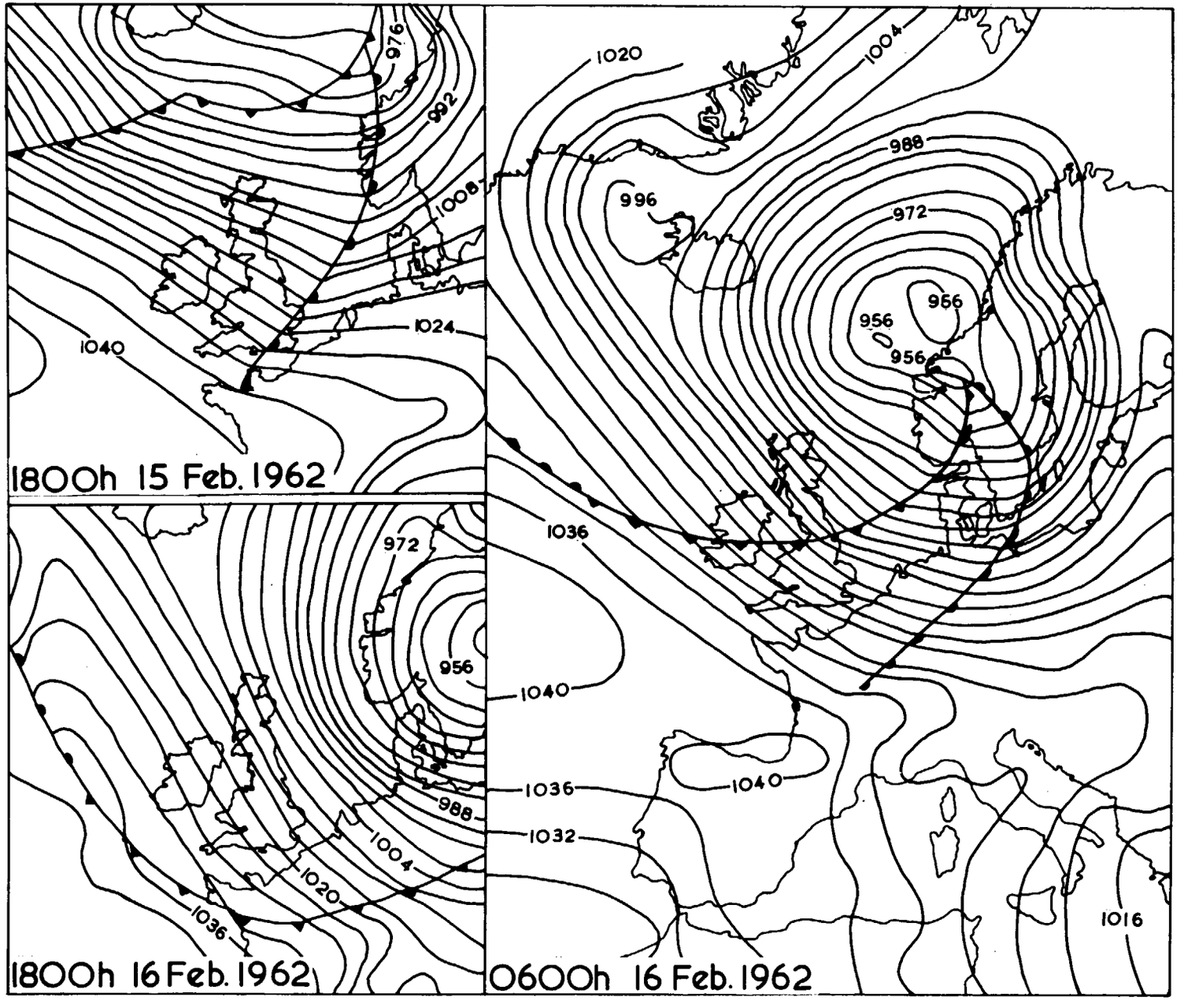

Figure 4: Weather charts for the storm surge of 15 to 17 February, 1962

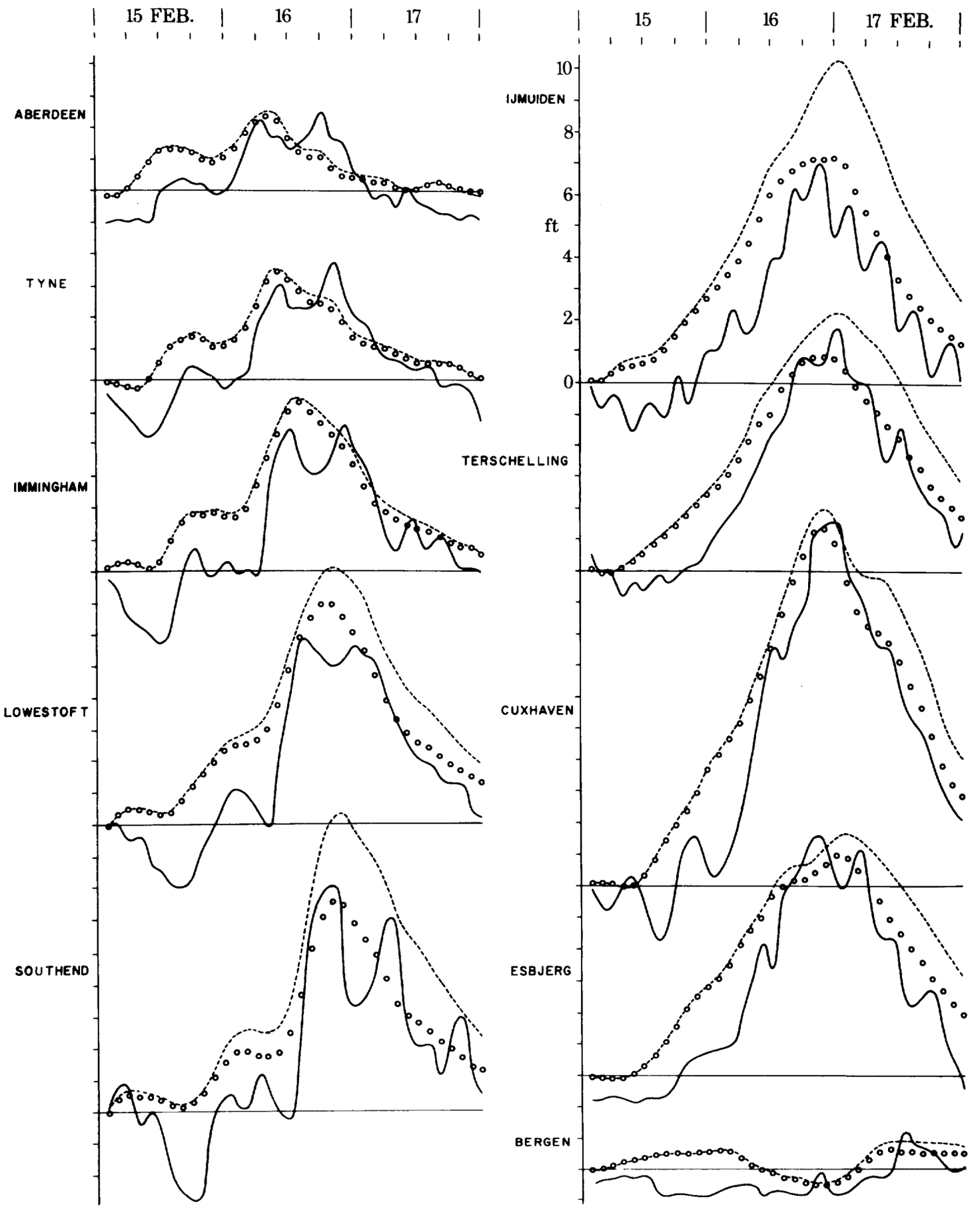

Figure 5: Storm surge of 15 to 17 February 1962 ; ——, residuals after removal of the barometric surge ;-----, wind surge from model 1 ; ○ , wind surge from model 2.

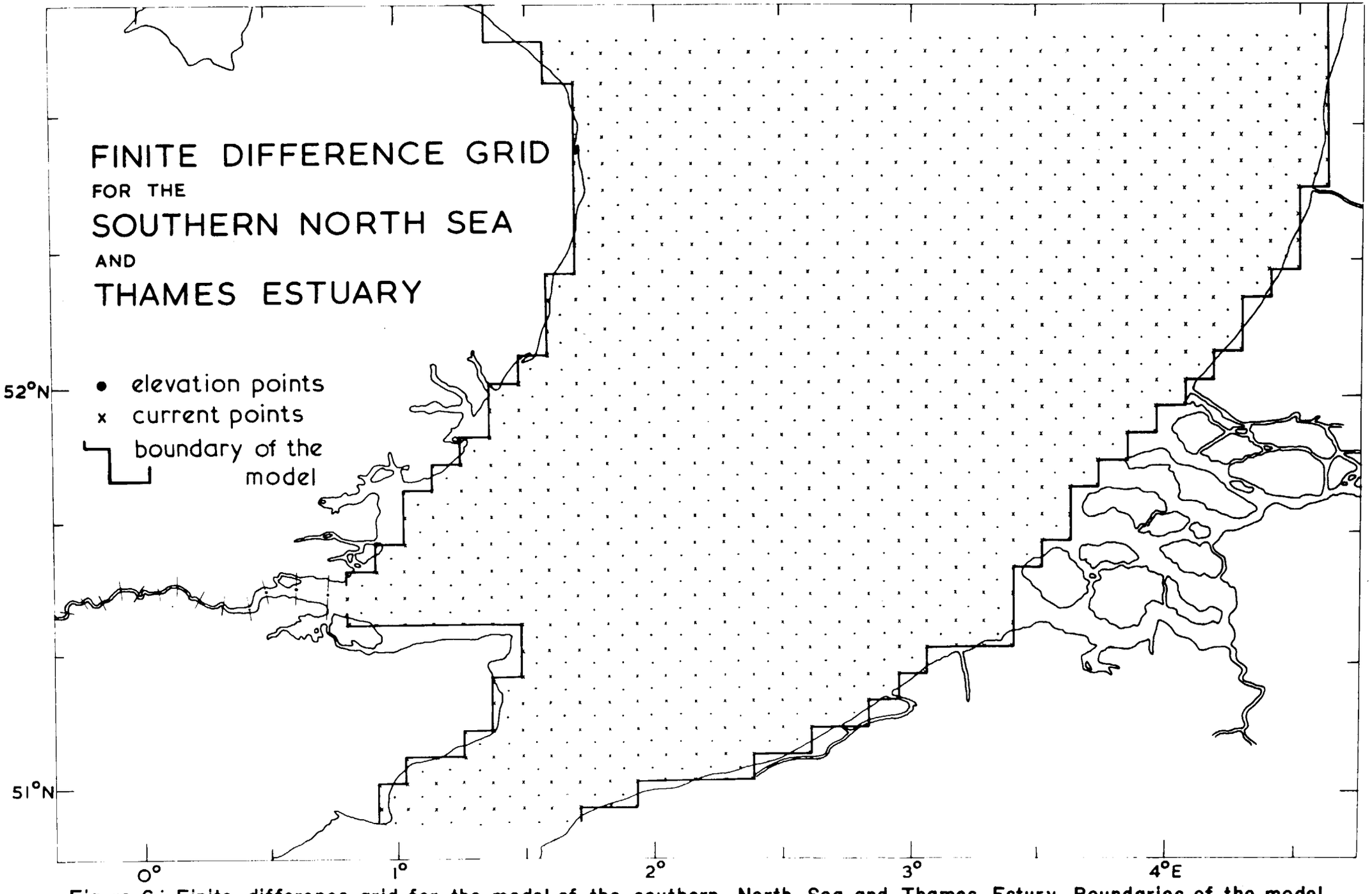

Figure 6: Finite-difference grid for the model of the southern North Sea and Thames Estury. Boundaries of the model marked on the grid: x—x, land boundaries; · · ·, open-sea boundaries. Sea levels are calculated at •, elevation points, and currents at ×, stream points; river elevations are calculated at –·–, elevation sections.

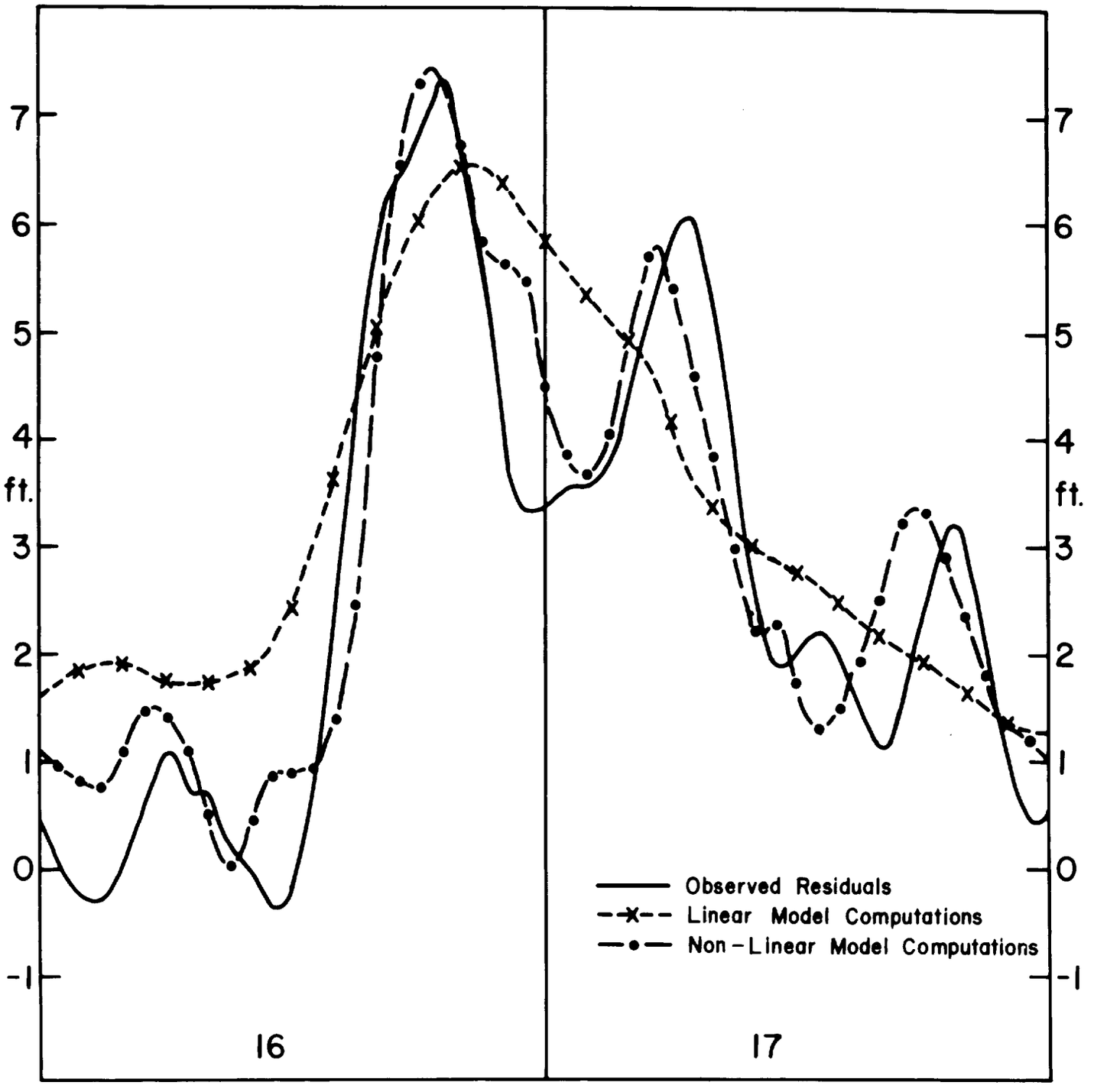

Figure 7. Wind-induced surge levels at Southend during the period of the Hamburg surge, 16 and 17 February 1962.——, Observed residual elevation after removal of the barometric surge; –•–, surge level ζ_{s+1} computed on the basis of wind and tide; –×–, wind surge ζ_s computed in the absence of tide.

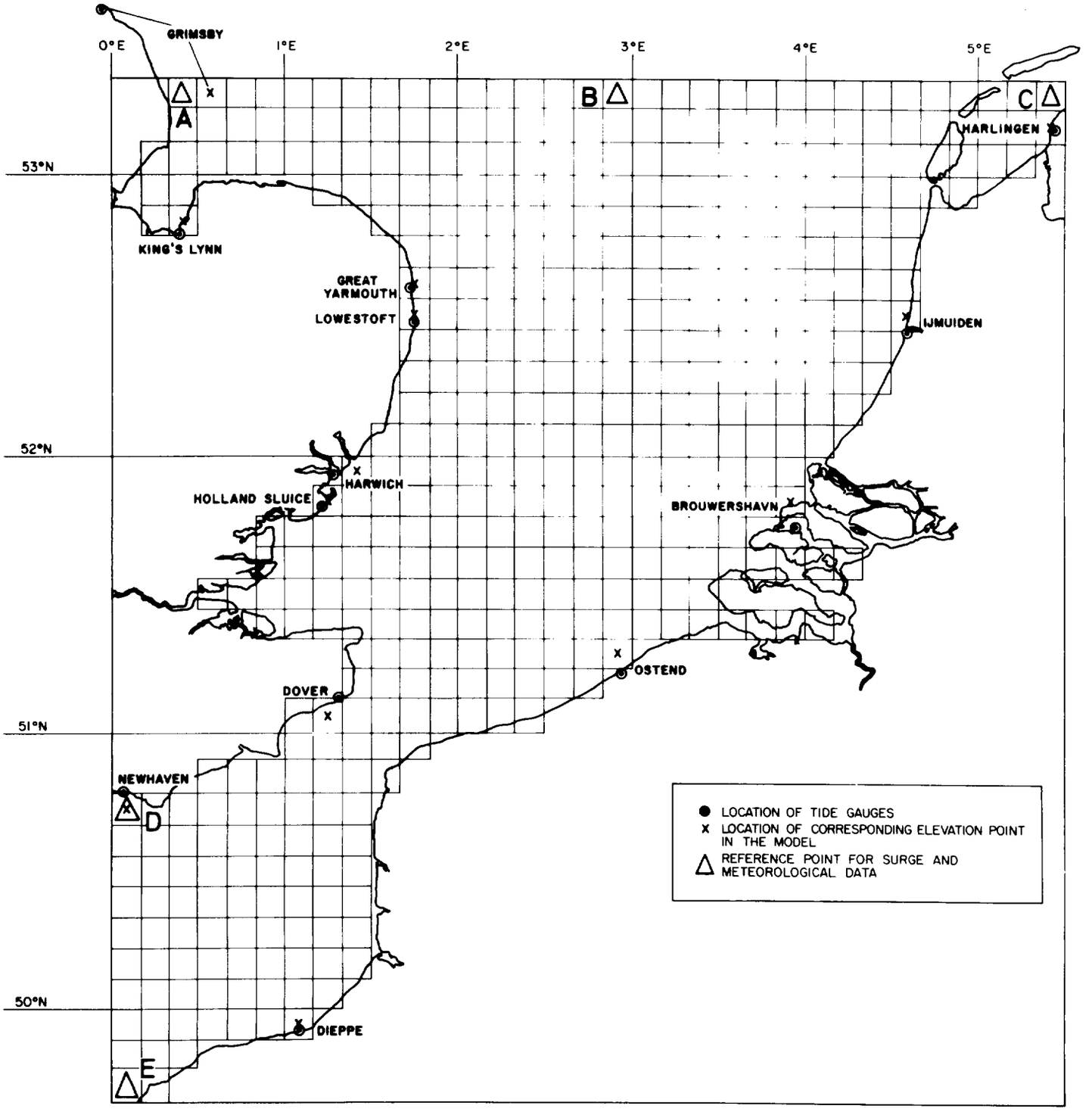

Figure 8: Schematic representation of the southern North Sea.

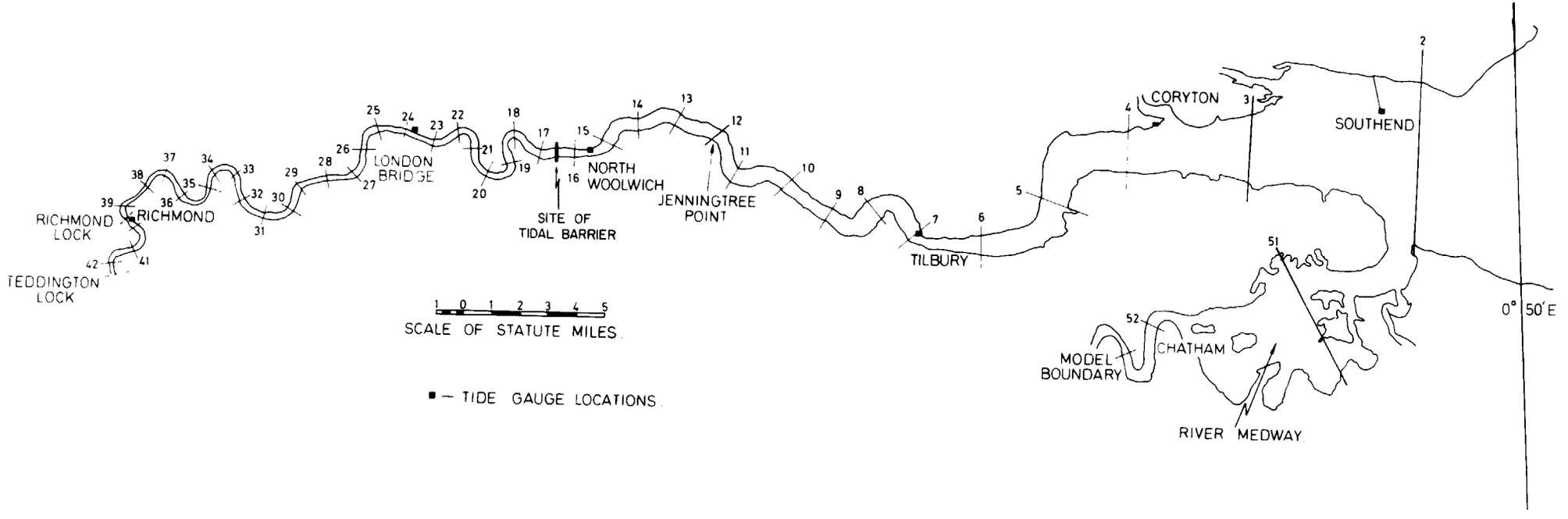

FIG 9: RIVER THAMES — SCHEMATIC REPRESENTATION.

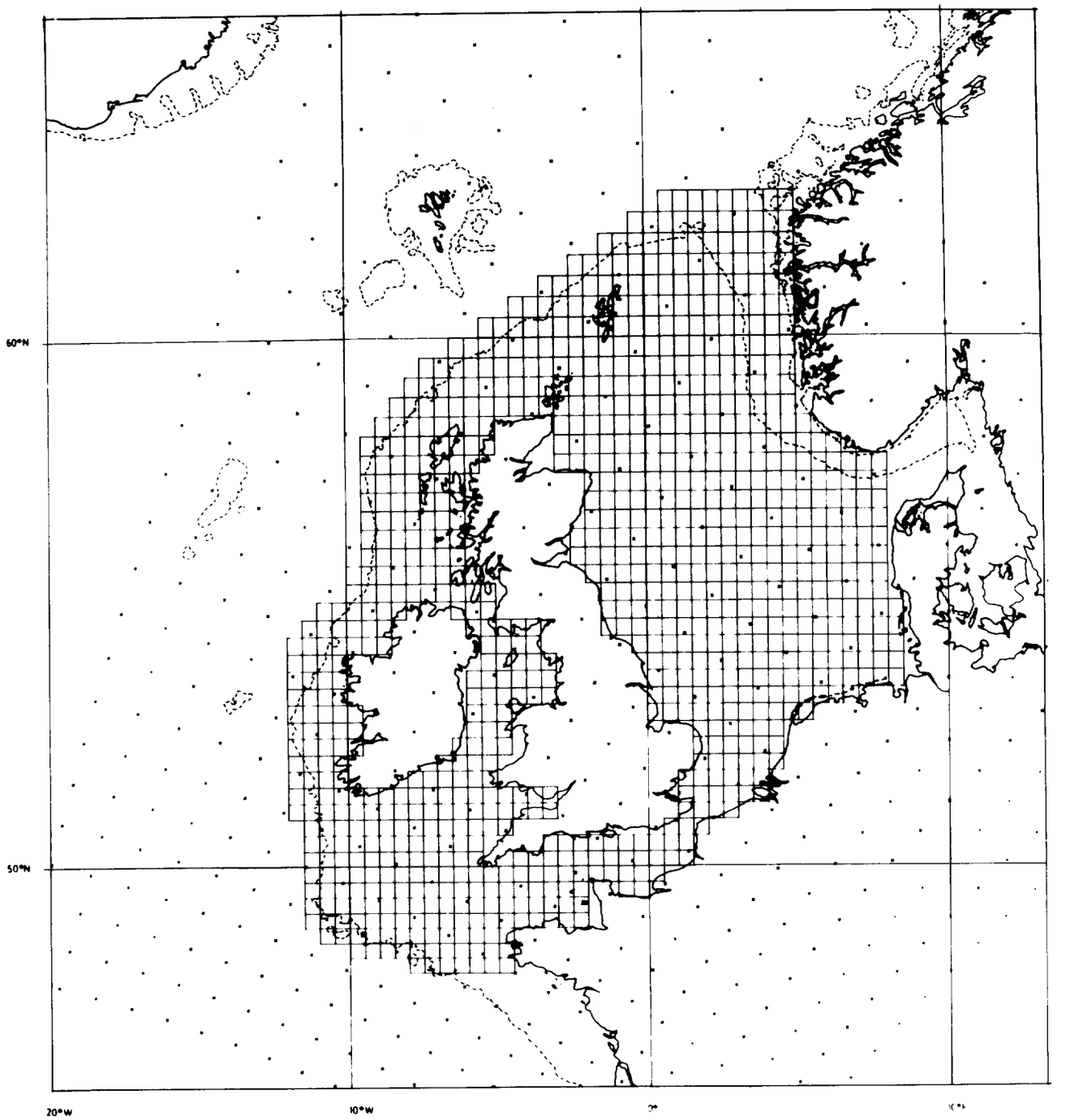

Fig 10: FINITE DIFFERENCE GRID FOR THE NORTH SEA AND CONTINENTAL SHELF USED IN STORM SURGE COMPUTATIONS WITH GRID POINTS OF THE 10-LEVEL METEOROLOGICAL MODEL (X), ----- 100 FATHOM DEPTH CONTOUR

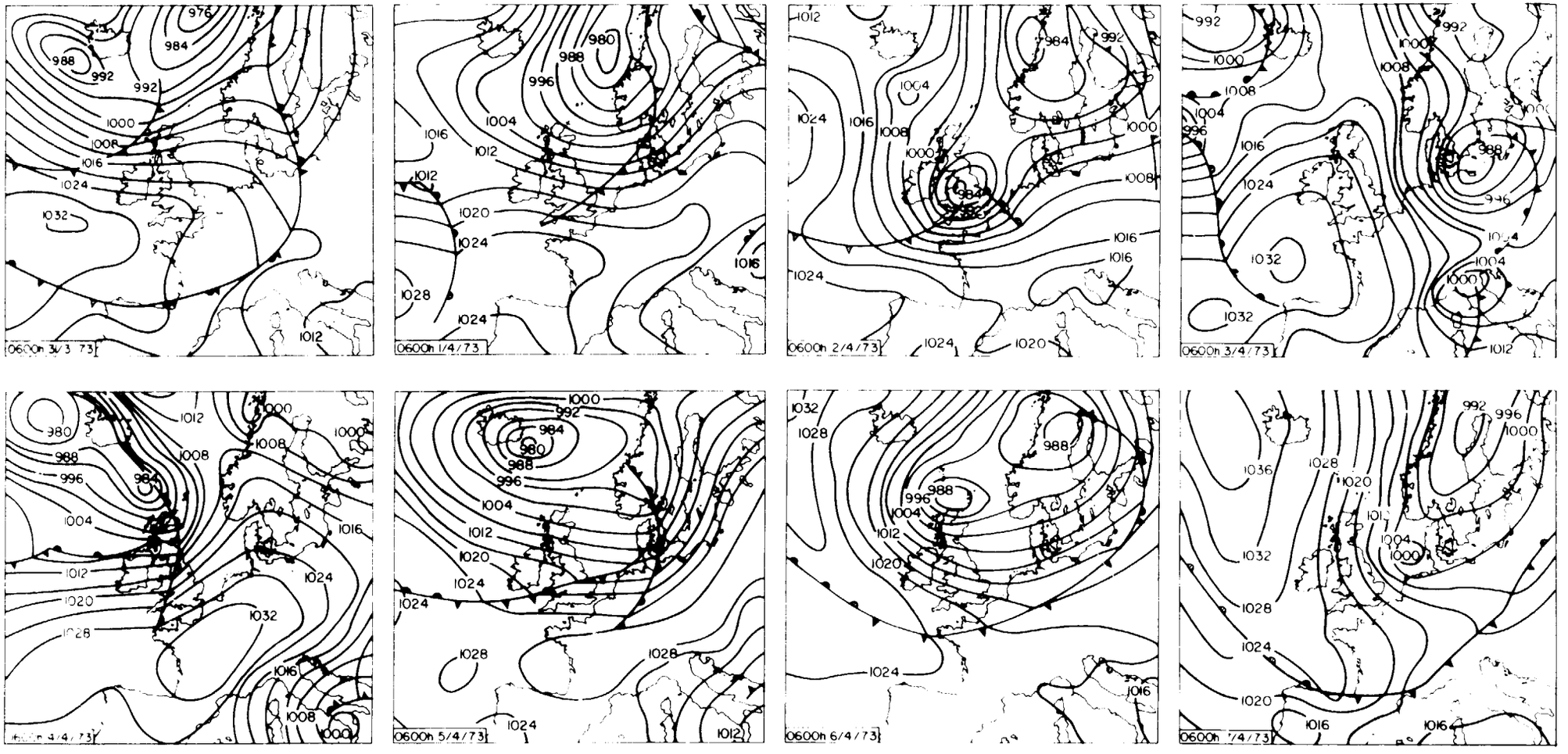

FIGURE 11: WEATHER CHARTS FOR THE STORM SURGE OF 1 TO 6 APRIL 1973

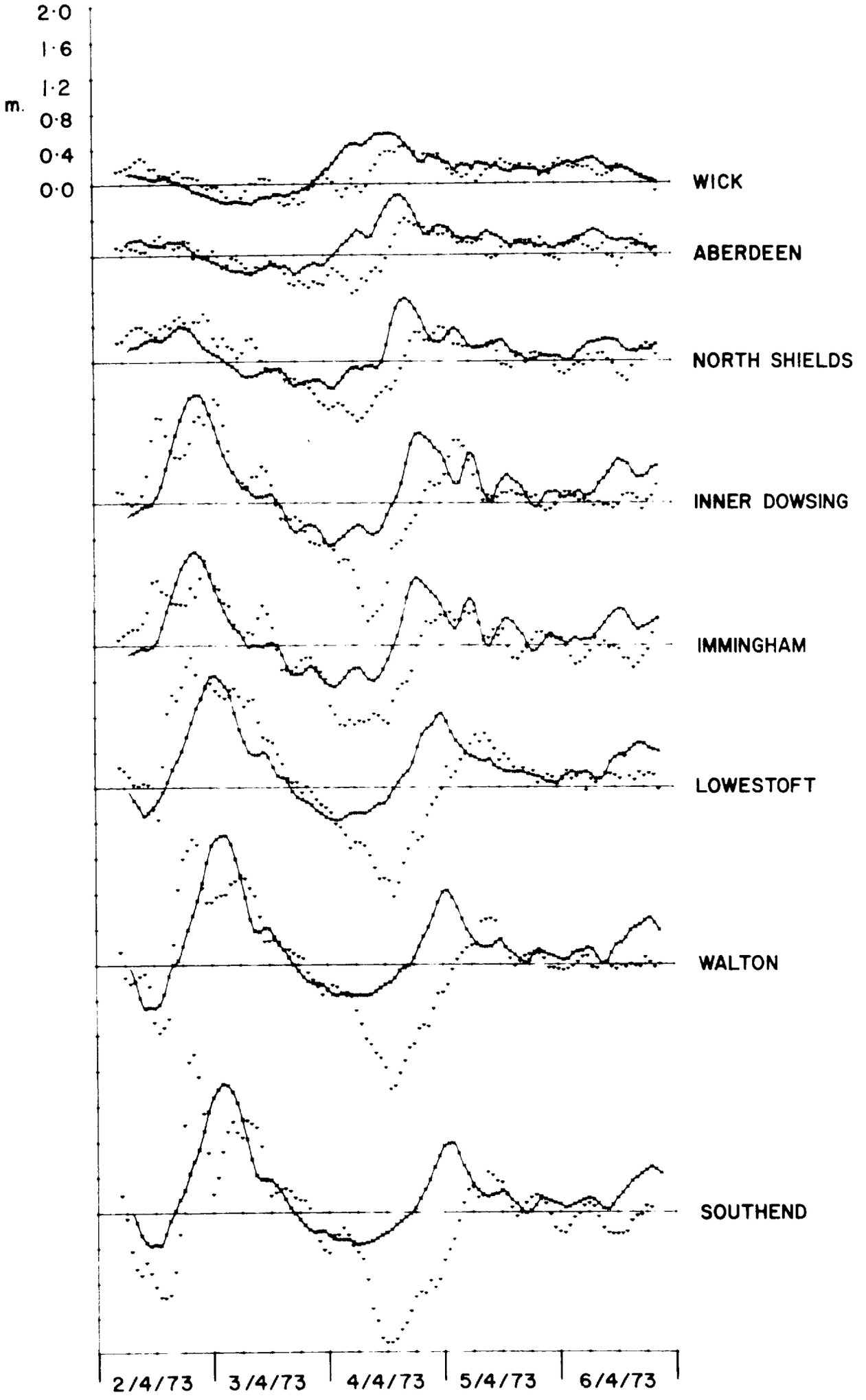

Figure 12a: Storm surge of 1-6 April, 1973 (English ports):
——— Computed; ▾▾▾▾▾ Observed.

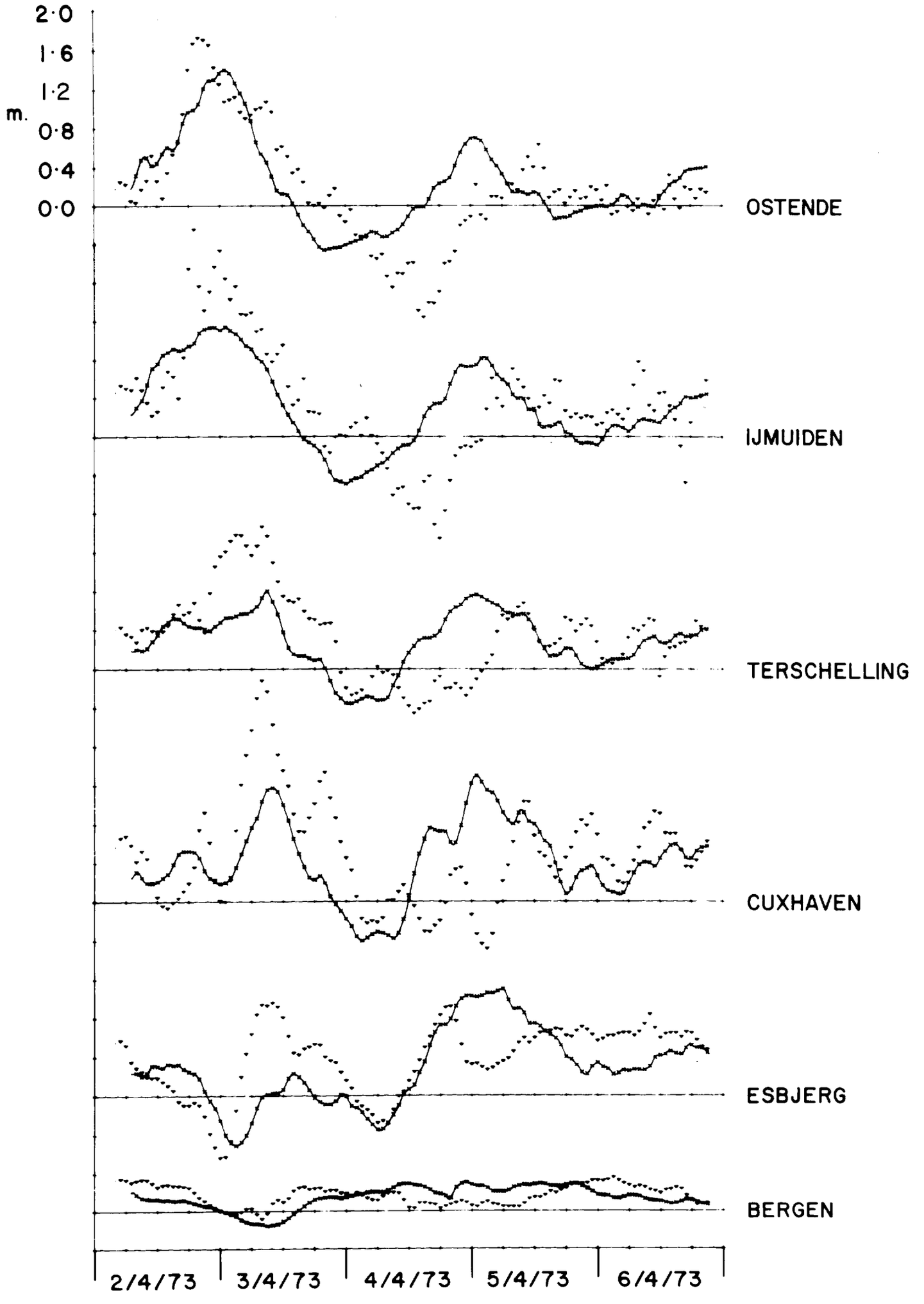

Figure 12b: Storm surge of 1-6 April, 1973 (Continental ports):
——— Computed; ▾▾▾▾▾ Observed.

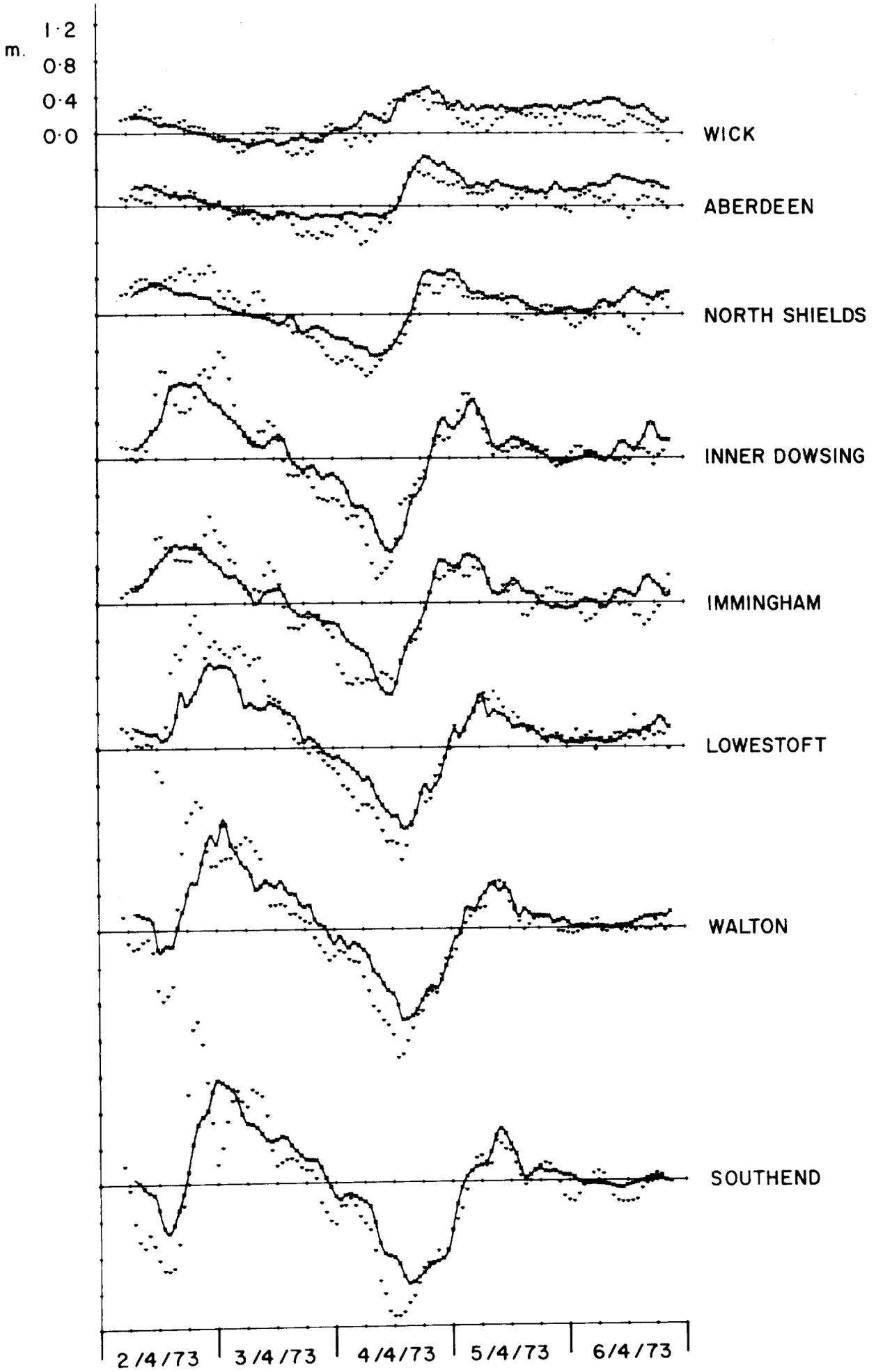

Figure 13a: Storm surges at UK ports ;
——— solution E ; ▾▾▾▾▾ observed.

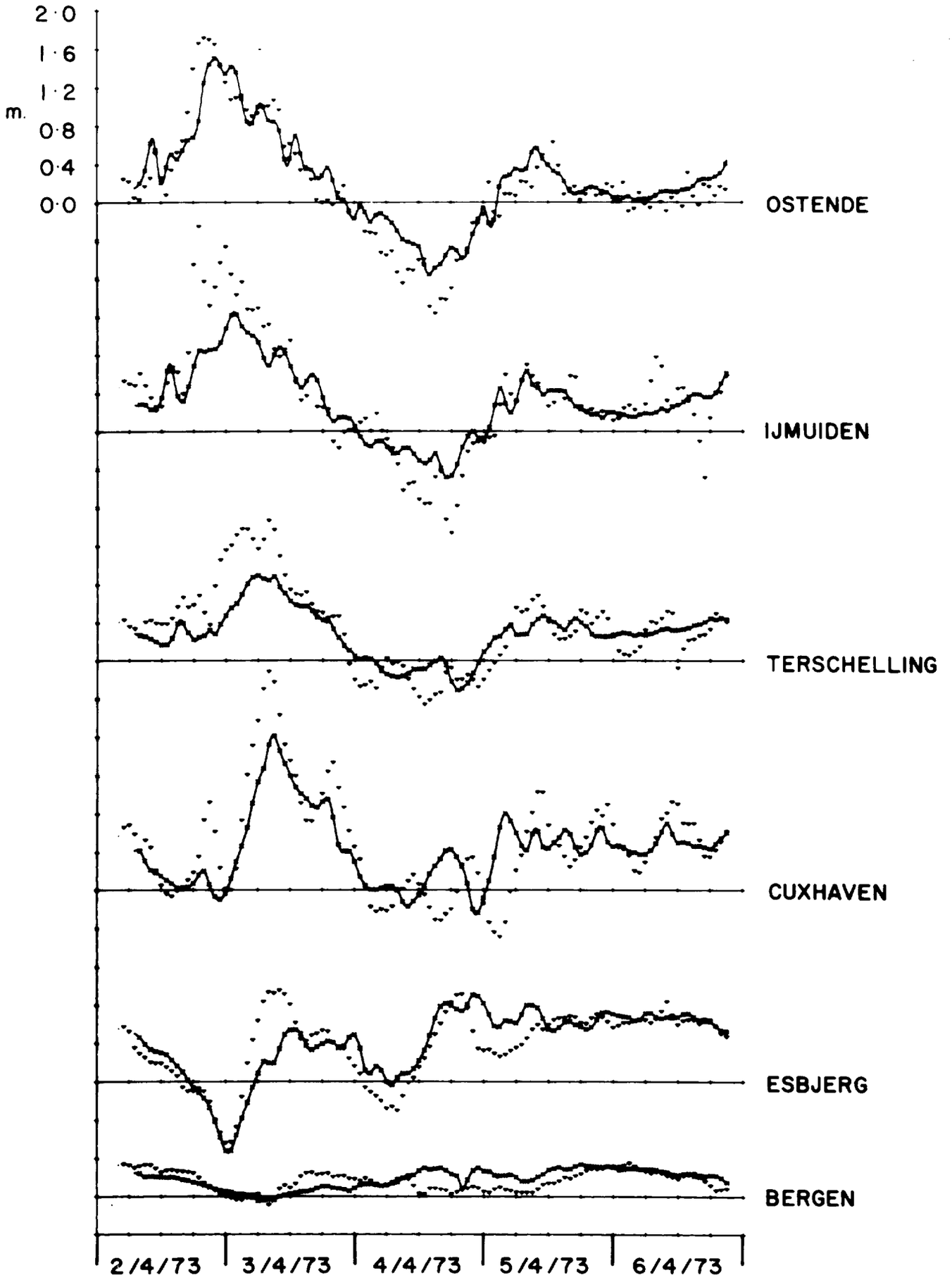

Figure 13b: Storm surges at continental ports;
—— solution E ; ▾▾▾▾▾ observed.

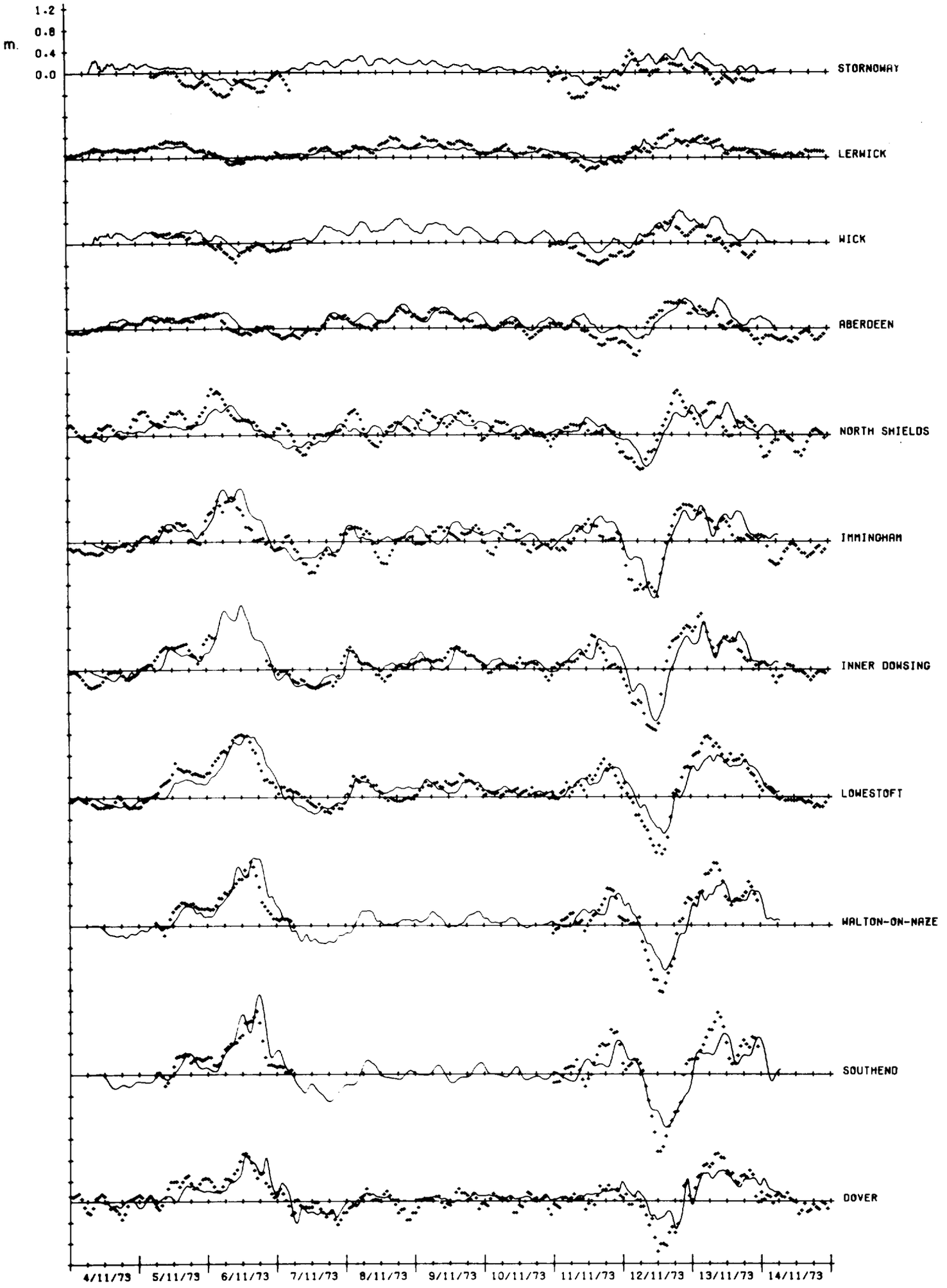

FIGURE 14a: STORM SURGES AT UK PORTS. COMPUTED (————): OBSERVED (++++++).

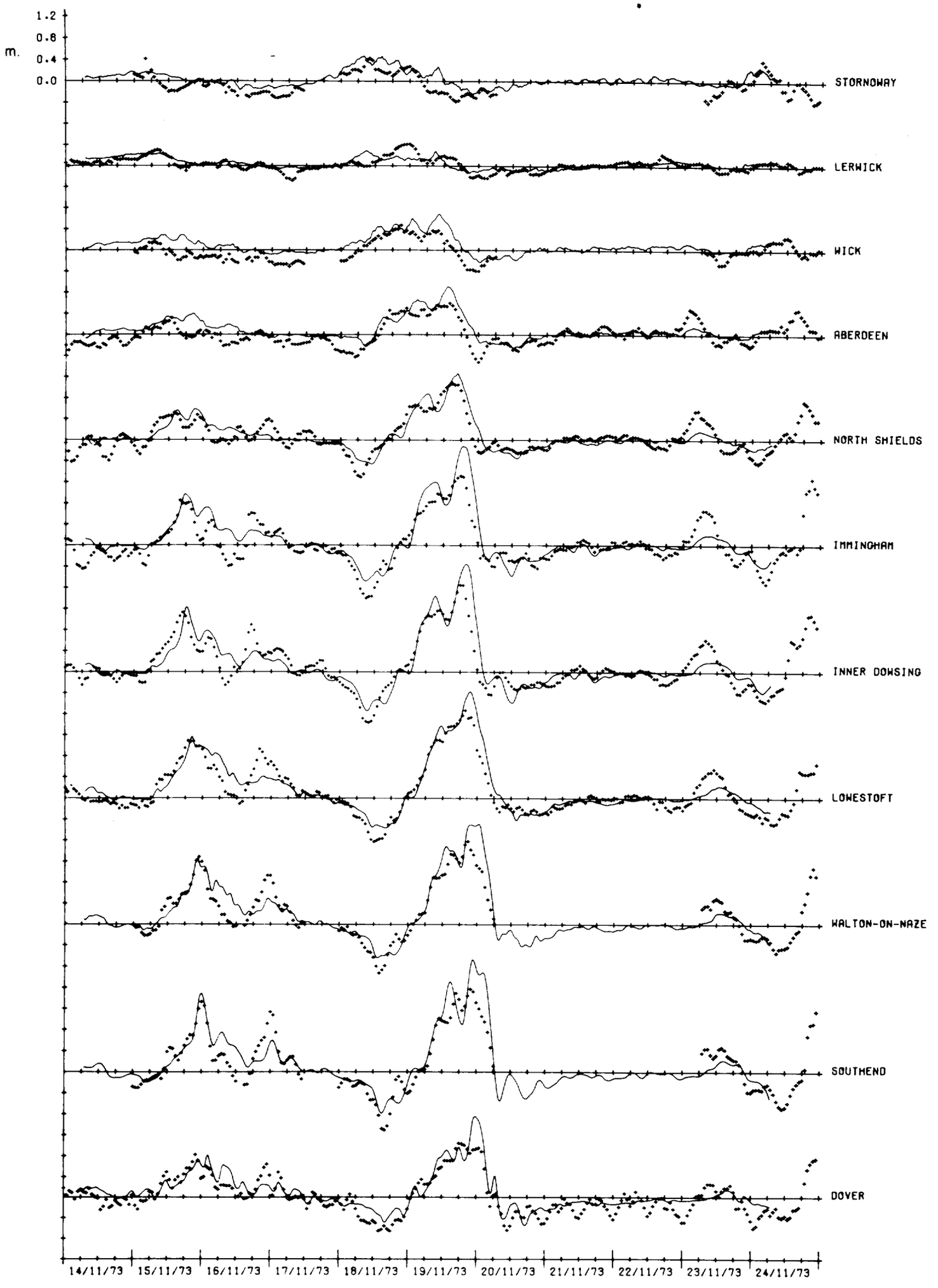

FIGURE 14b: STORM SURGES AT UK PORTS, COMPUTED (————); OBSERVED (++++++).

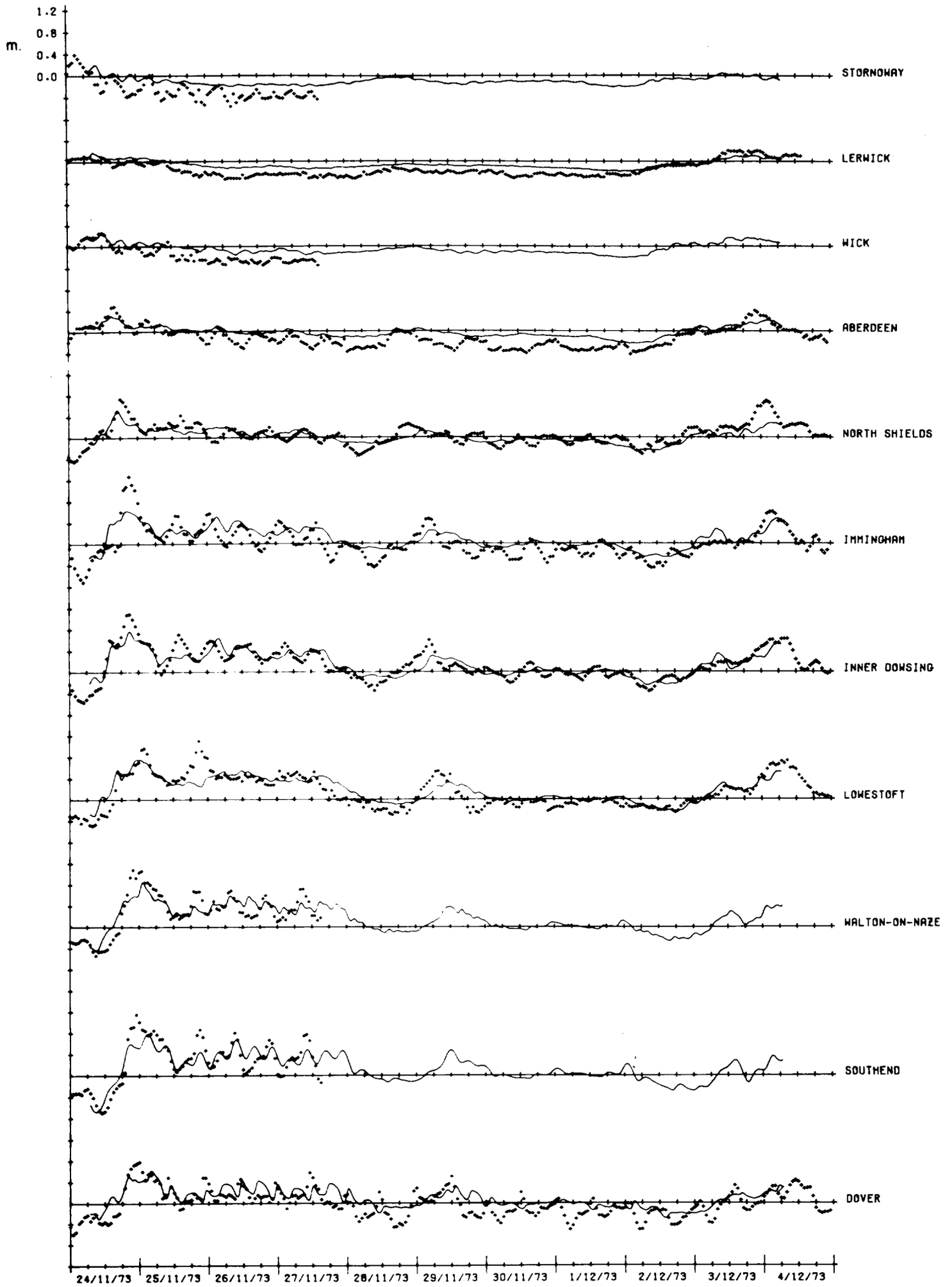

FIGURE 14c: STORM SURGES AT UK PORTS. COMPUTED (————): OBSERVED (++++++).

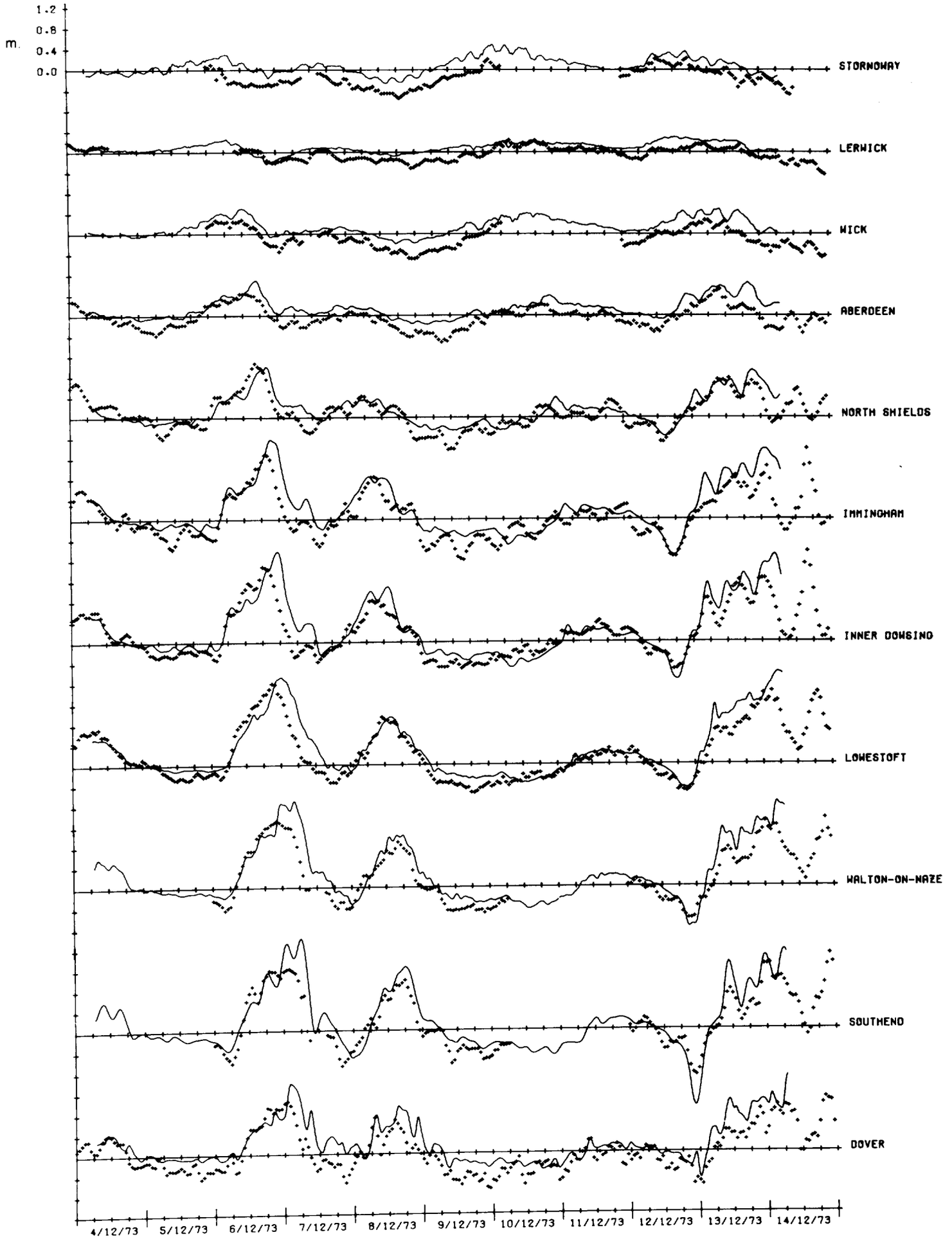

FIGURE 14d: STORM SURGES AT UK PORTS. COMPUTED (———); OBSERVED (++++++).

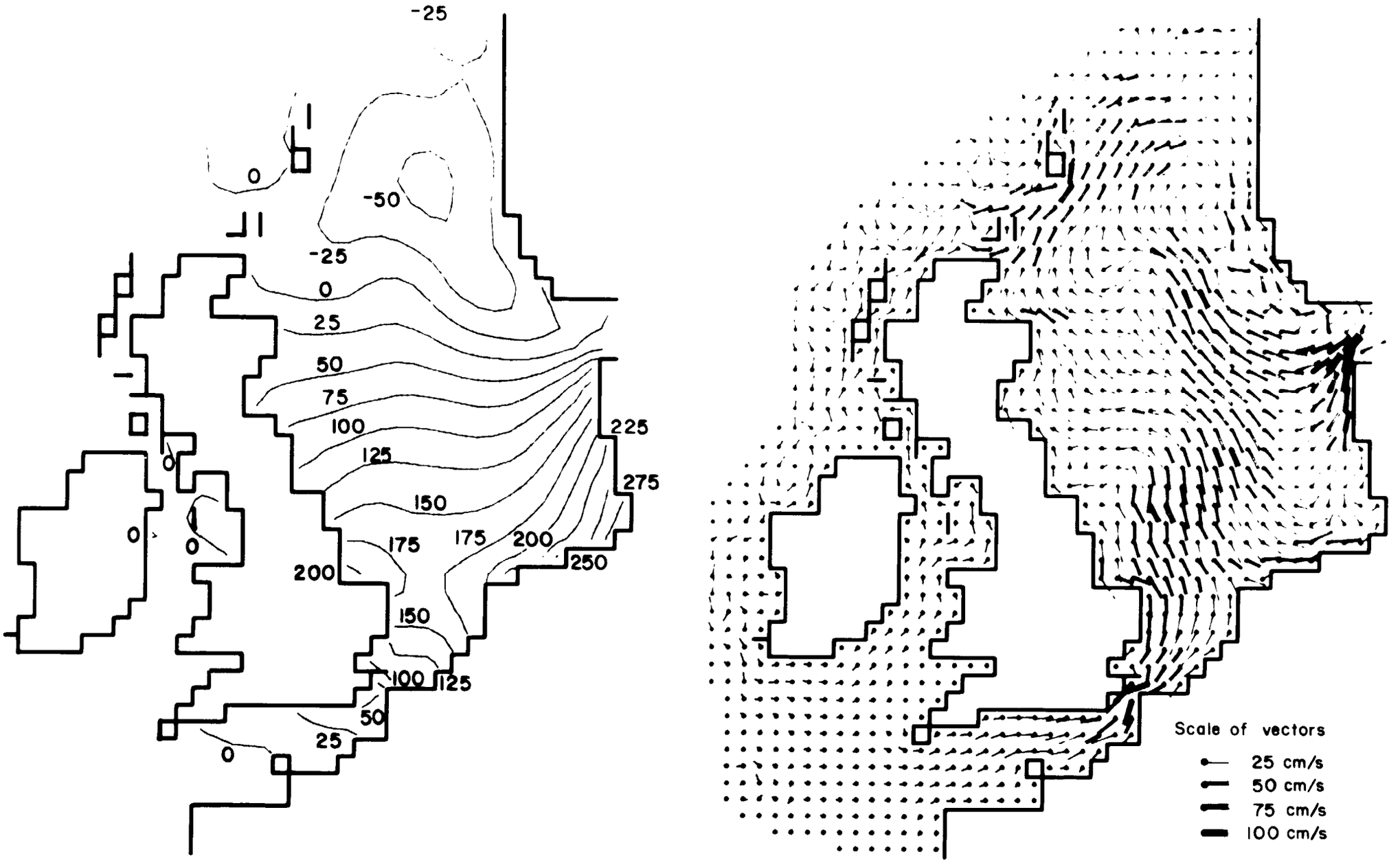

Figure 15 : The storm surge of 18-20/11/73. Contours of surface elevation (cm) and current vectors at

1900 19/11/73

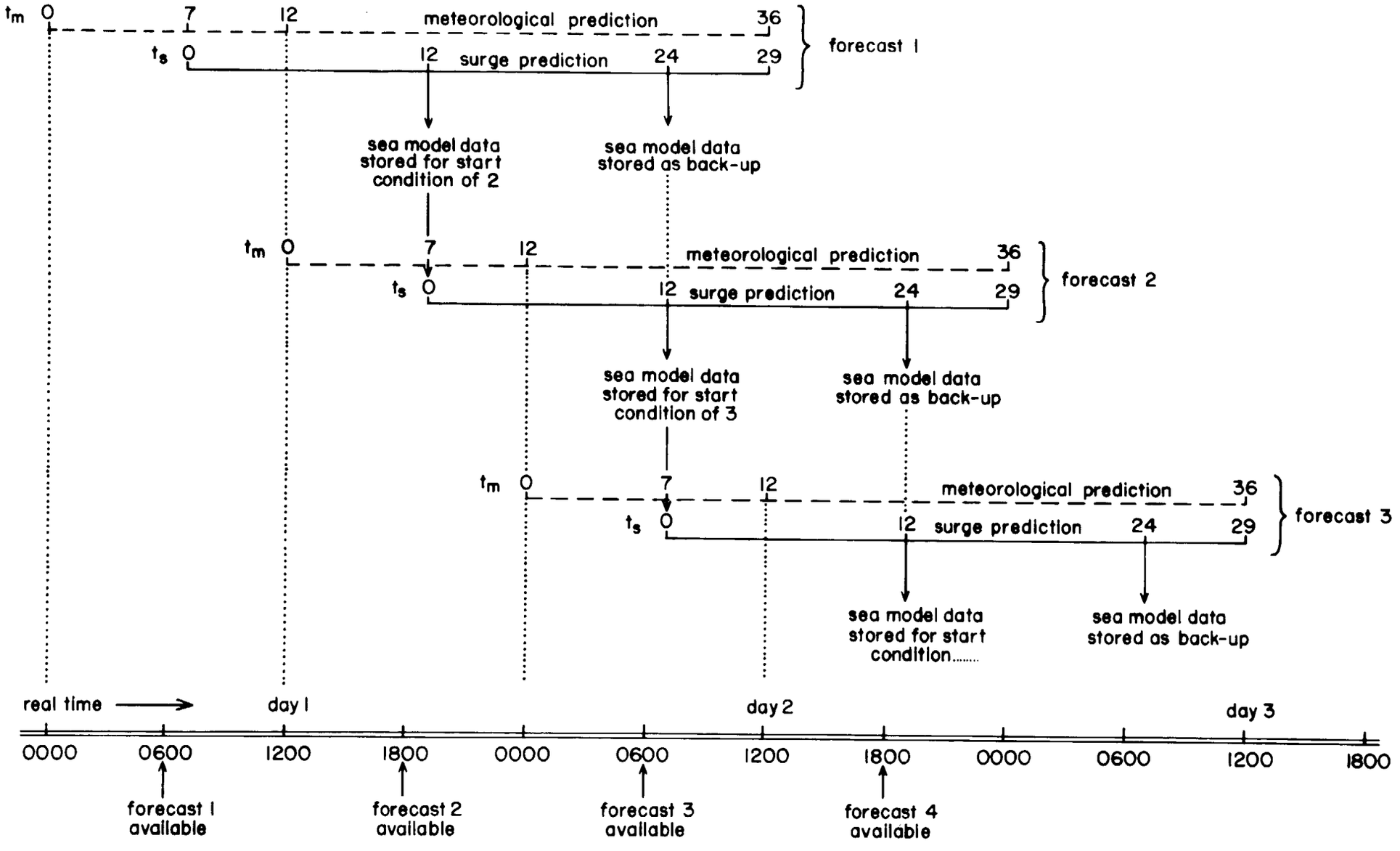

Figure 16: Scheme for operational surge forecasting providing overlapping predictions up to 30 hours ahead.

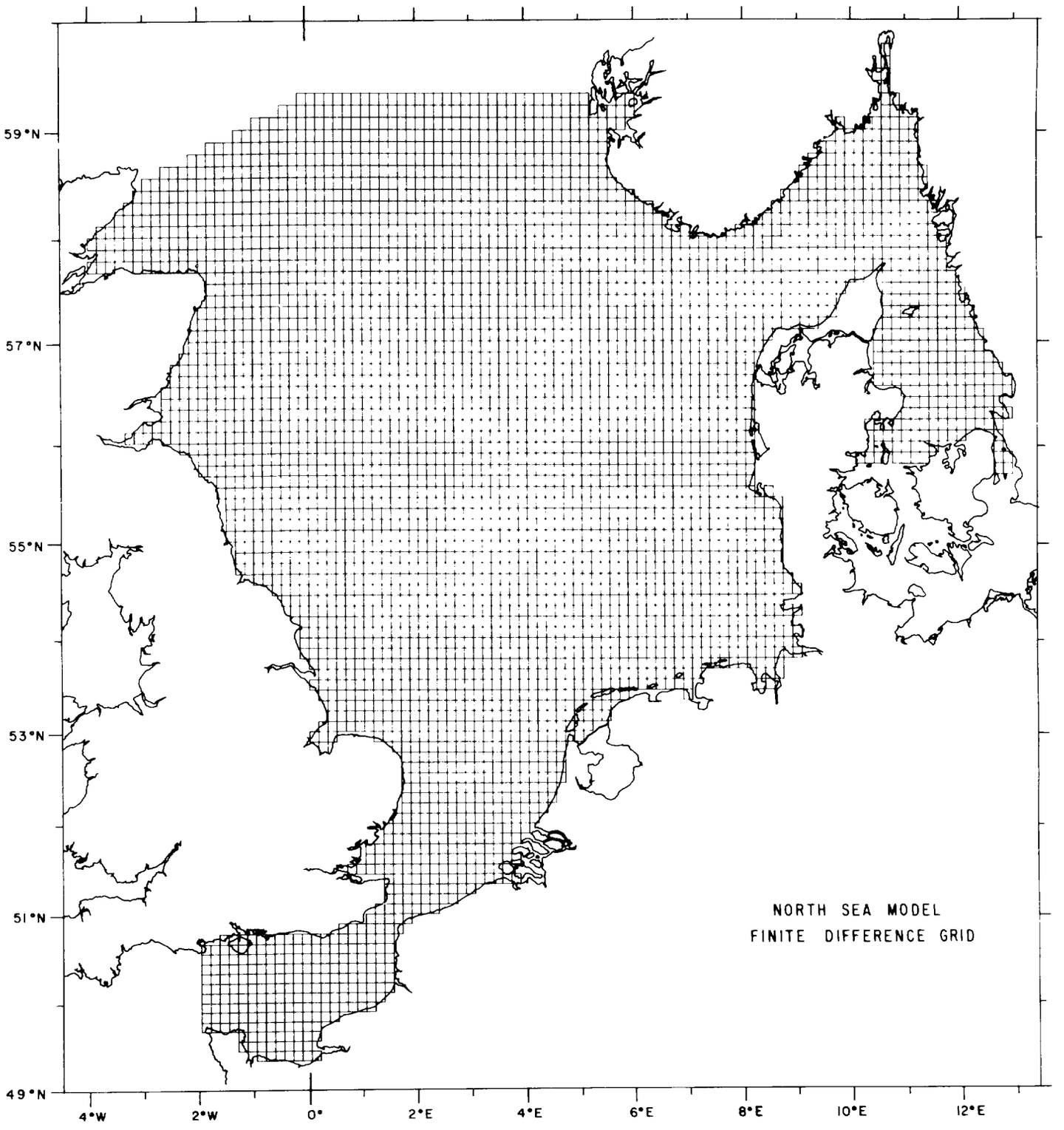

FIGURE 17: FINITE DIFFERENCE GRID OF NORTH SEA MODEL.

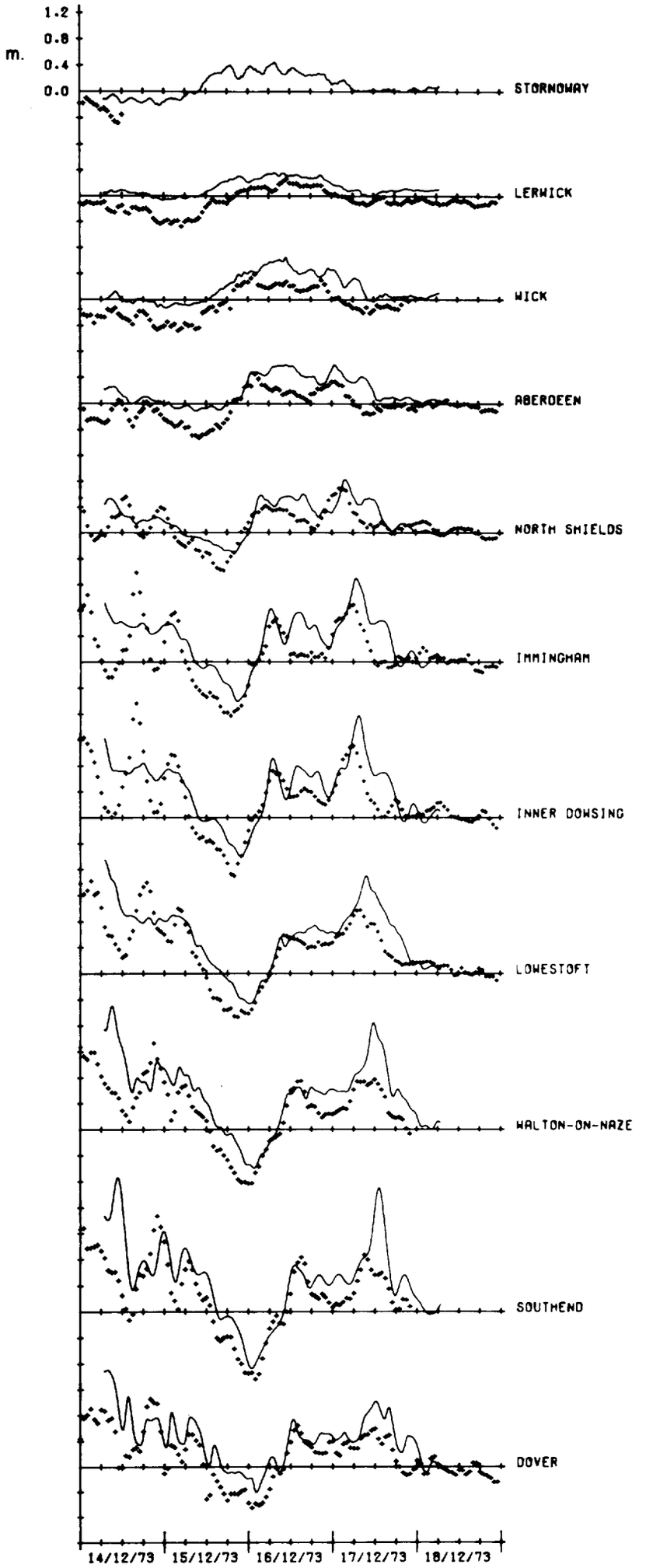

FIGURE 18a: STORM SURGES AT UK PORTS, COMPUTED (———); OBSERVED (++++++). RESULTS FROM THE SHELF MODEL.

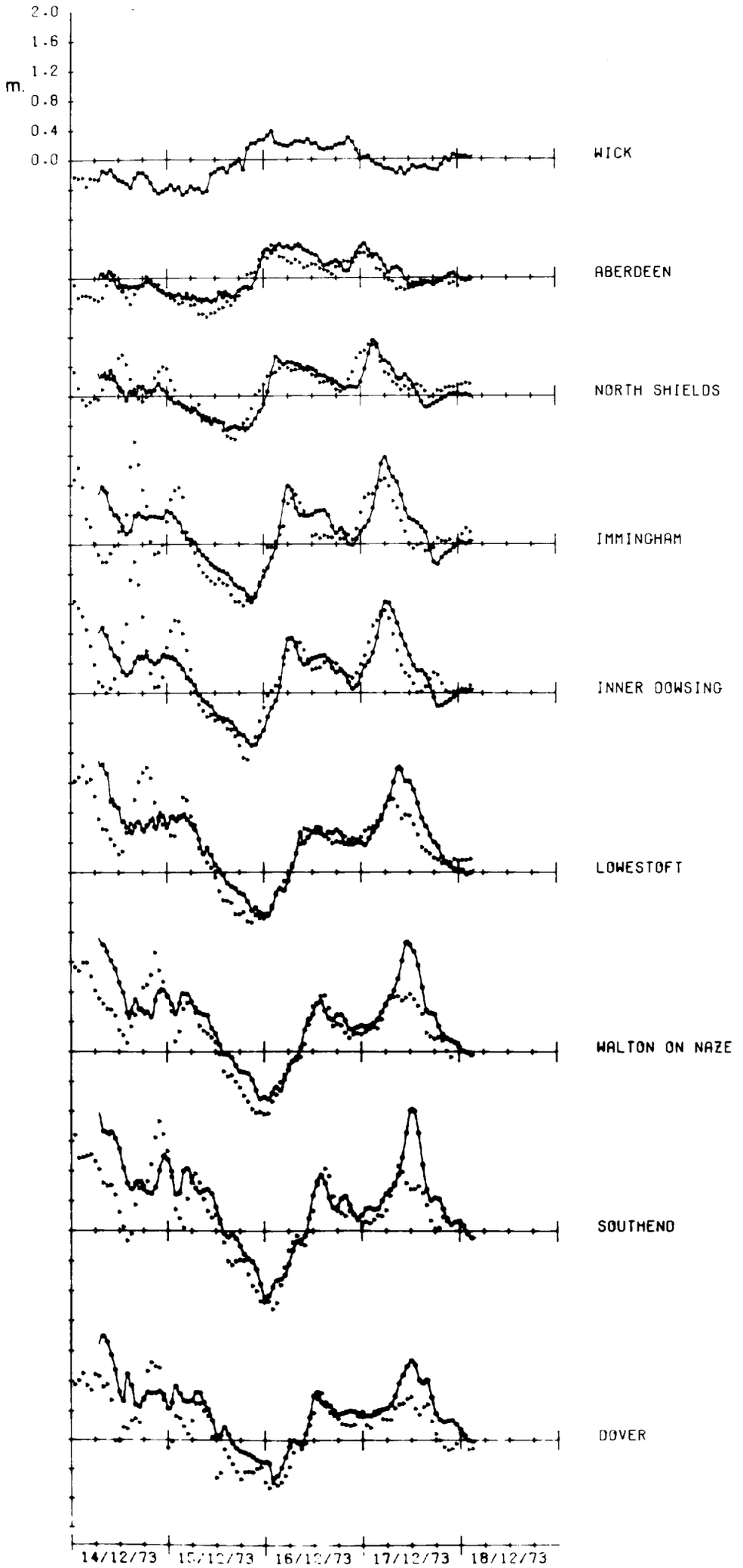

FIGURE 18b: STORM SURGES AT UK PORTS, COMPUTED (———) ; OBSERVED (+ + + +).
RESULTS FROM THE NORTH SEA MODEL.

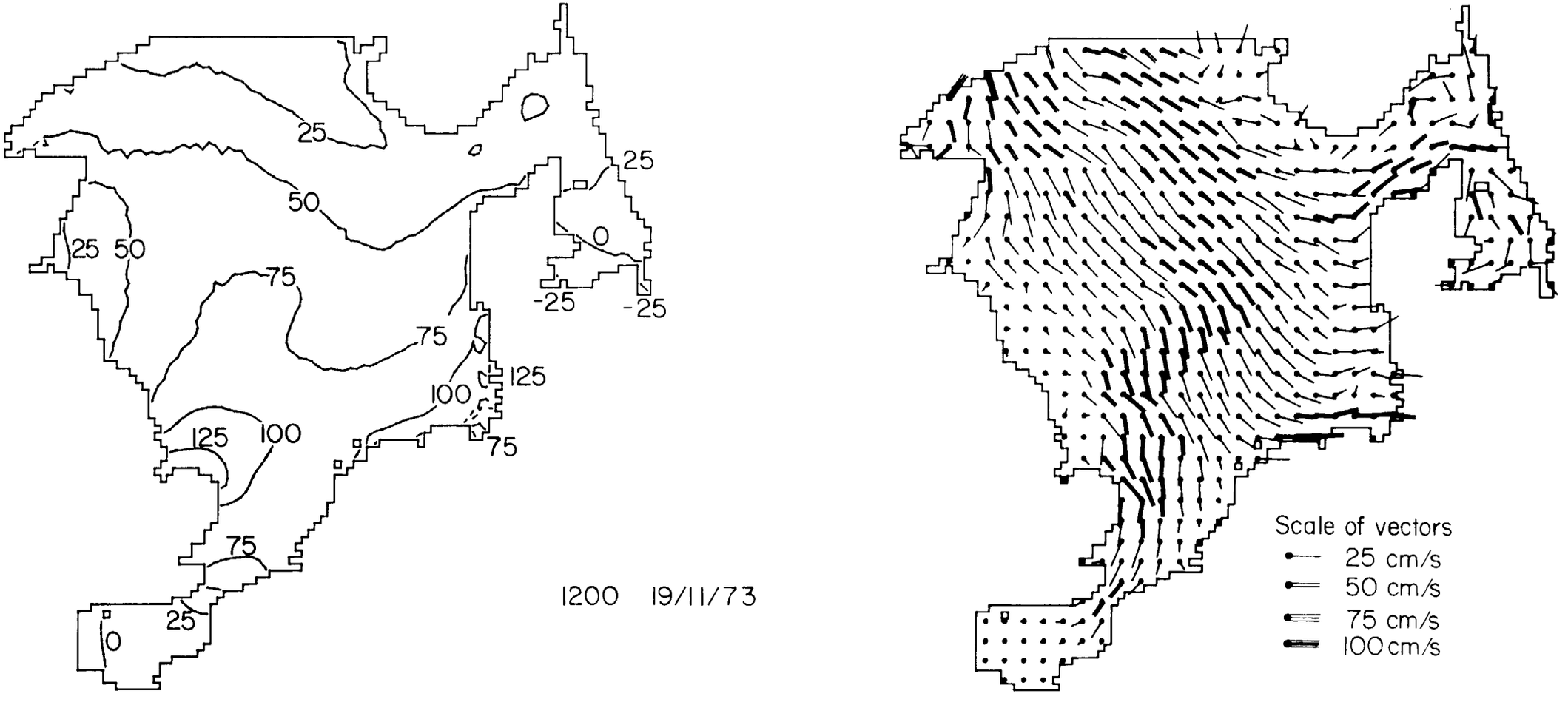

FIGURE 19: CONTOURS OF SURFACE ELEVATION (cm.) AND CURRENT VECTORS FOR THE STORM SURGE 19-20/11/73

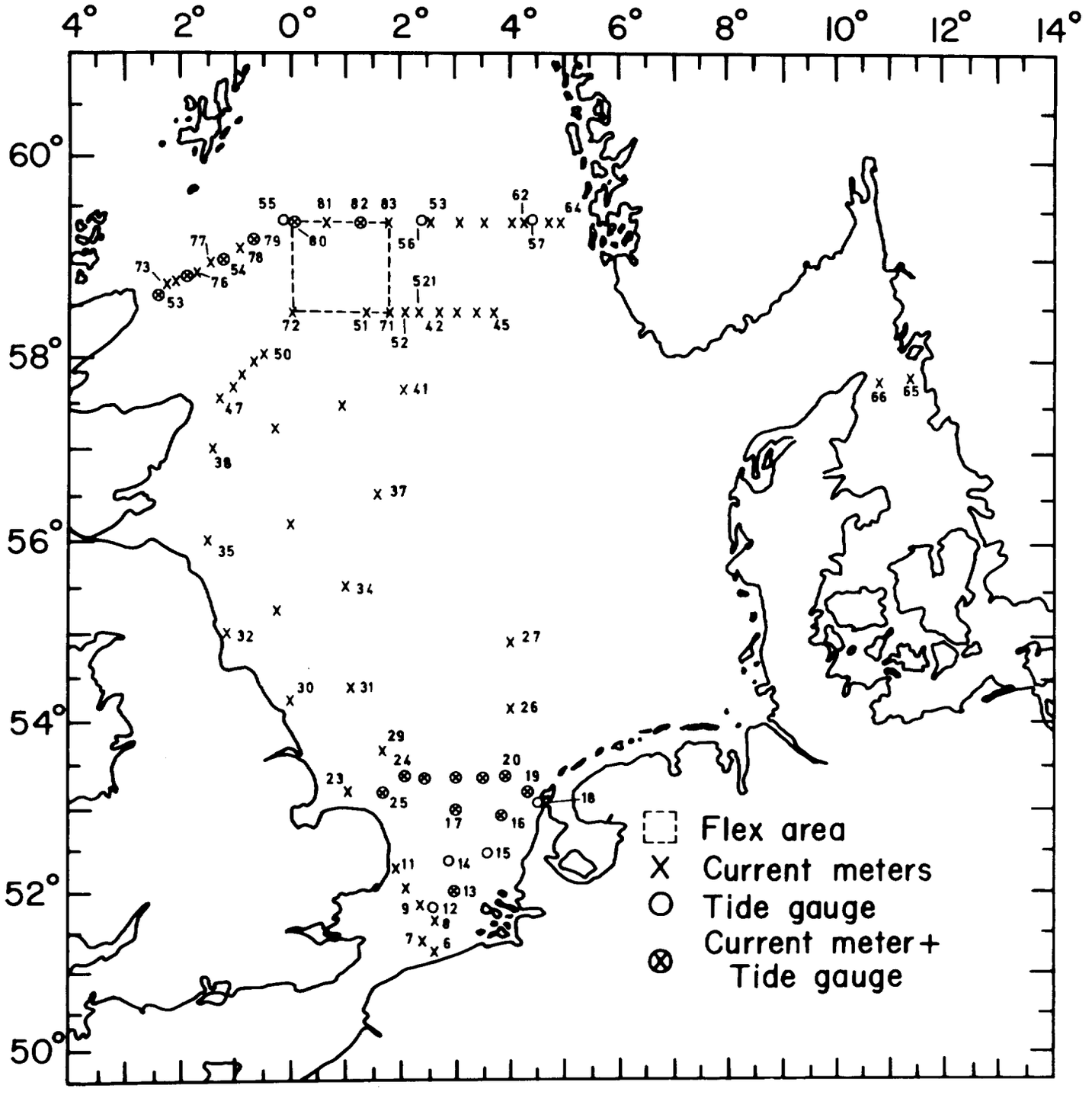

Figure 20: JONSDAP 76 "INOUT" moored network.

	Derivation	Period covered.	Model used.
A.	H_{1000} —hydrostatic law— p_a — ∇p_a — $\hat{\omega}$ —Hasse + Wagner (1971)— $\underset{\sim}{\omega}$ —C_D Heaps (1969)— $\underset{\sim}{\tau}^{(s)}$; ∇p_a interpolated; $\underset{\sim}{\tau}^{(s)}$ interpolated	26-30/3/1972 28/3-6/4/1973 4/11-18/12/1973 31/12/1975-6/1/1976	S S,N S,N S
B.	H_{1000} —hydrostatic law— p_a —interpolated— p_a — ∇p_a — $\hat{\omega}$ —Hasse + Wagner (1971)— $\underset{\sim}{\omega}$ —C_D Heaps (1969)— $\underset{\sim}{\tau}^{(s)}$	31/12/75-6/1/76	S
C.	H_{1000} —hydrostatic law— p_a —interpolated— p_a — ∇p_a; (U_{1000}, V_{1000}) —assume = $\underset{\sim}{\omega}$ —interpolated— $\underset{\sim}{\omega}$ —C_D Heaps (1969)— $\underset{\sim}{\tau}^{(s)}$	31/12/75-6/1/76	S,N
D.	H_{1000} —hydrostatic law— p_a —interpolated— p_a — ∇p_a — $\hat{\omega}$; h'_{950} —interpolated— h'_{950} — $\bar{T}_{950}$ — T_a —+ ICES T_s data— ΔT_{a-s}; $\hat{\omega}$ + ΔT_{a-s} —Hasse (1974)— $\underset{\sim}{\omega}$ —C_D Heaps (1969)— $\underset{\sim}{\tau}^{(s)}$	31/12/75-6/1/76	S,N
E.	as C but with C_D from Smith + Banke (1975)	31/12/75-6/1/76	S
F.	as E but with 'NORSWAM' data (p_a, $\underset{\sim}{\omega}$) over the North Sea	31/12/75-6/1/76	S,N
G.	as B but starting from p_a	29/3-2/4/1977	S
H.	as C but starting from p_a and $\underset{\sim}{\omega}$	29/3-2/4/1977	S
I.	as D but starting from p_a and T_a	29/3-2/4/1977	S

☁ = information supplied by Met. Office ; □ = data input to sea model ;

S = continental shelf model , N = North Sea model.

Figure 21 : Derivation of input data for storm surge calculations, storm periods covered and models used.

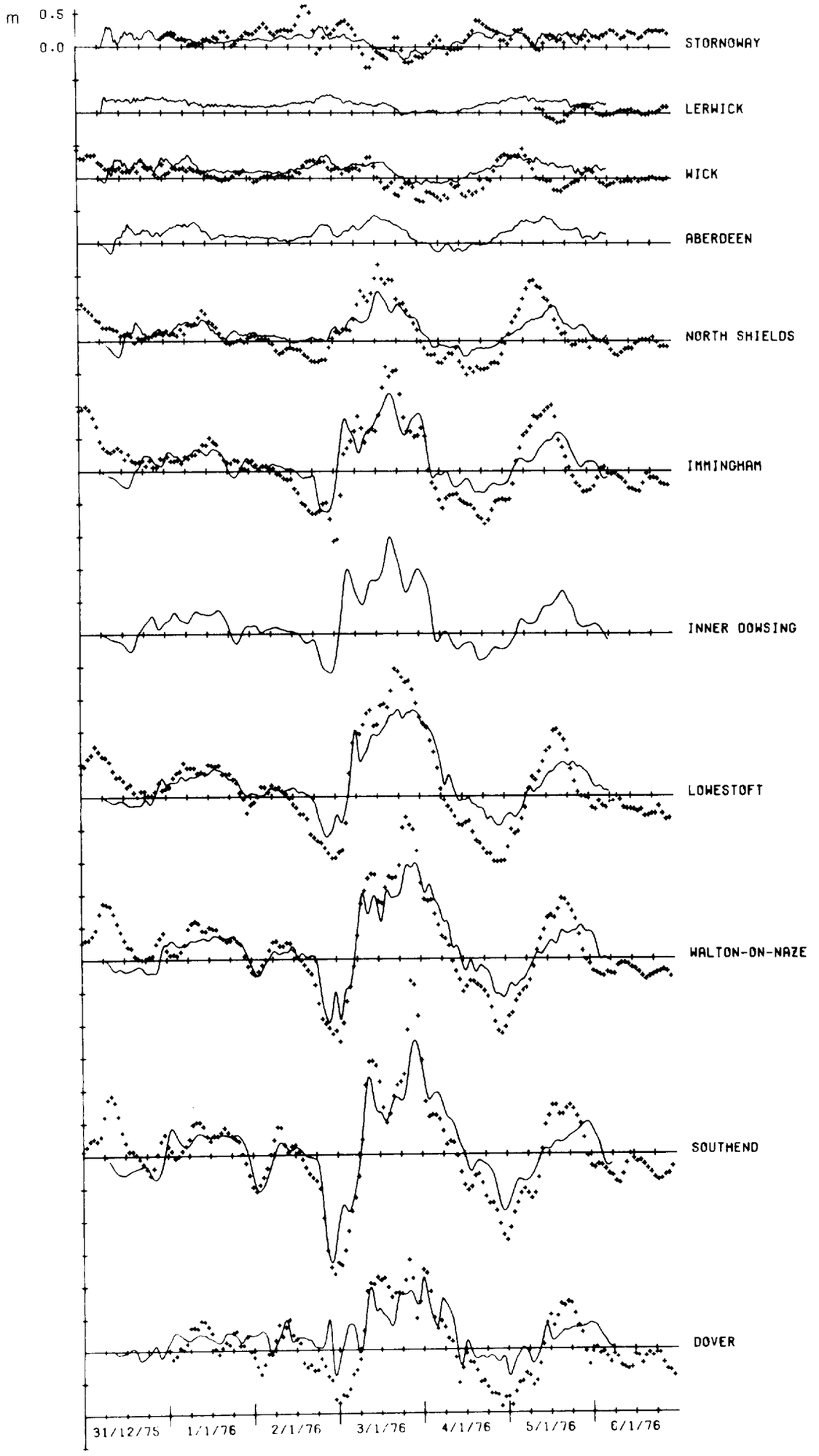

FIGURE 22: STORM SURGES AT UK PORTS. COMPUTED (———): OBSERVED (++++++). USING PROCEDURE B, §8.

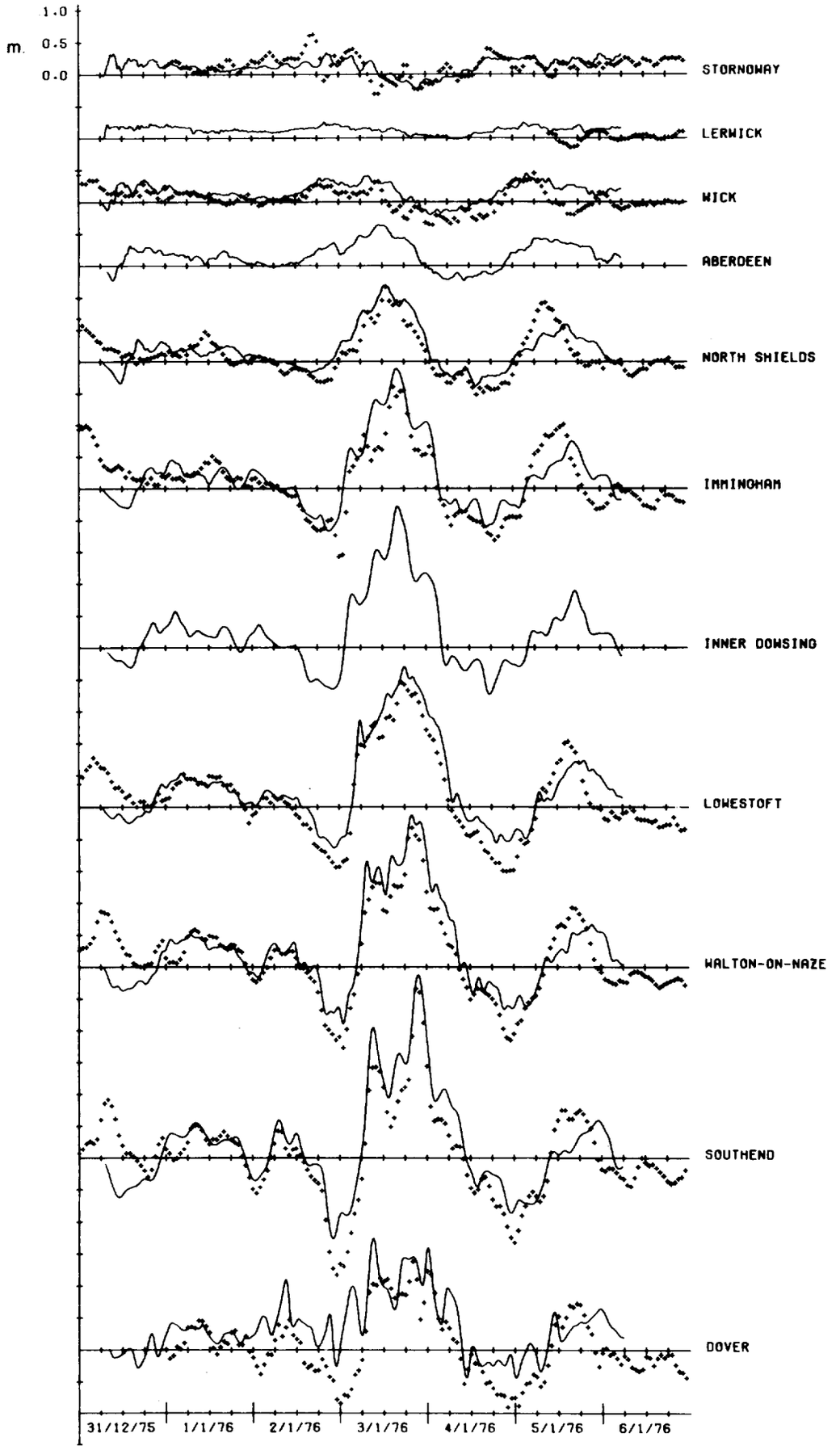

FIGURE 23: STORM SURGES AT UK PORTS. COMPUTED (————); OBSERVED (++++++).
USING PROCEDURE F, §8.